

Zusammenfassung Chapter01 and 02 a

Donnerstag, 23. Juni 2022 17:33

I. Introduction

I.1 Introduction to nanoscience

Nanoscience is the science in nm-scale.

I.2 SI-Einheiten

- [s]: Is defined via the frequency $\Delta\nu_c$ for which a C^{133} Atom is oscillating between two energy-states
- [m]: Is defined via the speed of light
- [kg]: Is defined via the Planck-constant h expressed in $\frac{kg\cdot m^2}{s}$
- [A]: Is defined via the elementary charge e expressed in $C = A \cdot s$
- [K]: Is defined via k_B in $3K^{-1} = kg\cdot m^2\cdot s^{-2}\cdot K^{-1}$
- [mol]: Is defined via N_A in mol^{-1}
- [Cd]: Is defined via luminous efficacy of monochromatic radiation of frequency

II. Electronic properties of nanostructures

Following chapters:

- Description of charge transport in bulk materials (single crystals/disordered systems) and the temperature dependence of charge carrier mobilities
- Physics of surfaces & interfaces (DOS & electronic bands) formation of space charge layers and properties of pn-junctions
- Working principle of (opto-)electronic devices
- Conductance in low-dim. systems
- Role of quantization effects in electronic transport

II.1 Theoretical description of charge transport

Literatur: p.23

II.1.1. Drude model

For extrinsic conductivity (charge carrier concentration $n \neq n(T)$)
the current density \vec{j} (caused by an external field) can be calculated by:

$$\vec{j} = ne\vec{v}_D$$

In the Drude model, \vec{v}_D is given by:
$$\boxed{\frac{d}{dt}(mv_D^\rightarrow) + \frac{m\vec{v}_D^\rightarrow}{\tau_m} = e\vec{E}}$$

with $\langle \tau_m \rangle$: average relaxation time of charge carriers to come back to equilibrium (friction caused by thermal vibrations of atoms)

In steady state ($\frac{d}{dt} m \vec{v}_D = 0$) and low fields: $\vec{v}_D \propto$ field

\Rightarrow Def. proportionality constant m (mobility):

$$m = \frac{e}{m} \langle \tau_m \rangle$$

$$\Rightarrow \vec{j} = \sigma \vec{E} \quad \text{with } \sigma = n e m = \frac{n e^2}{m} \langle \tau_m \rangle$$

$\sigma = \sigma(T) \Rightarrow$ four different cases

1. Intrinsic: Carriers are generated by thermal excitation
2. Extrinsic: Carriers are generated by introducing dopants
3. Injection controlled: Carriers are injected at electrodes
4. Photoconductivity: Carriers generated by absorption of light

Now: motion of e^- in the VB of a perfect SC with applied field:

Equation of motion of a single e^- in k-space:

$$\vec{F} = -e \cdot [\vec{E} + \vec{v} \times \vec{B}] = m \frac{d\vec{k}}{dt}$$

If the e^- moves to the 1.BZ, an "Umklapp"-process takes place

$\lceil e^- \text{ re-enters in 1BZ} \rfloor$

This process happens as long as the field is not high enough, where the e^- transits to the next empty band.

\lceil For higher fields, the Zener tunneling occurs. \rfloor

With the eff. mass, the band structure can be included:

$$\frac{1}{m^*} = \frac{1}{\hbar^2} \left(\frac{d^2 E}{dk^2} \right)^{-1} \Rightarrow E = \frac{\hbar^2 k^2}{2m^*}$$

Drude model with band structure:

$$m = \frac{e}{m^*} \langle \tau_m \rangle$$

\lceil If $m^* > m \Rightarrow m(m^*) < m(m)$ e.g. organic/inorganic SC \rfloor

II. 1.2 Boltzmann's Transport equation & drift diffusion model

Literature: p. 25

• BTE: Charge transport in highly crystalline systems with free electron gas

Describe the probability of finding one e^- at $t, \vec{r}, \vec{k} \pm d\vec{k}$ with $f(\vec{r}, \vec{k}, t)$

\lceil At equilibrium and in absence of ex. fields:

$$f = \text{Fermi-Dirac}$$

- Any disturbance leads to BTE:

$$\frac{df}{dt} = \frac{\vec{E}_t}{\hbar} \nabla_{\vec{k}} f(\vec{k}) + \vec{v} \nabla_{\vec{r}} f(\vec{k}) - \frac{\partial f}{\partial t}$$

change of distr. function
due to the force of the field

$$\vec{E}_t = \vec{E} + \vec{v} \times \vec{B}$$

\rightarrow Drift of charge carriers

Change due to
concentration
gradients

\rightarrow Diffusion of
charge carriers

Local change

BTE describes how the initial distr. Function changes with time due to:

drift ($-\frac{df}{dt}$), diffusion & collision ($\frac{df}{dt}$)

Sometimes hard to solve \rightarrow drift diffusion model

- Drift diffusion model:

1. Electrons as classical particles
2. Charge carriers in local equilibrium
3. All dopants ionized
4. Electrical current as result of:
 - Drift under applied field
 - Diffusion from high ChCa. concentrated regions to lower ChCa

1. Drift contribution

$$\vec{j}_n = q n M_n \vec{E}, n: \text{density}$$

2. Diffusion contribution

$$\vec{j}_{\text{diff}} = q D \vec{\nabla} n, \text{Diff. const. } D, \text{ concentrationgrad. } \vec{\nabla} n$$

$$\Rightarrow \vec{j}_n = q n M_n \vec{E} + q D \vec{\nabla} n \quad \text{and} \quad \vec{j}_p = q p M_p \vec{E} + q D \vec{\nabla} p$$

Drift, diffusion \Rightarrow no common Fermi energy

\Rightarrow Quasi-Fermi level: Concentrations

$$n_c(\vec{r}, T) = N_c(T) \exp\left(-\frac{E_c(\vec{r}) - E_{F,n}(\vec{r})}{k_B T}\right), \quad p_v(\vec{r}, T) = N_v(T) \exp\left(-\frac{E_{v,p}(\vec{r}) - E_v(\vec{r})}{k_B T}\right)$$

N_c, N_v : DOS in VB, CB

Change in quasi-Fermi-levels:

$$\nabla E_{F,n}(\vec{r}, T) = \nabla E_c(\vec{r}) + k_B T \frac{\nabla \ln n_c(\vec{r}, T)}{n_c(\vec{r}, T)}$$

↑
" " for $\nabla E_{F,p}$

In total:

$$\vec{j} = \vec{j}_n + \vec{j}_p = \vec{E} + \vec{v} \times \vec{B} + \frac{q}{m} \vec{\nabla} \Phi + \frac{q}{m} \vec{\nabla} \Phi$$

In total:

$$\vec{j} = \vec{j}_{\text{drift}} + \vec{j}_{\text{diff}} = [\sigma_n(T) + \sigma_p(T)] \vec{E} + \frac{k_B T}{q} \left[\frac{\sigma_n}{n_c} \nabla n_c - \frac{\sigma_p}{p_v} \nabla p_v \right]$$

II.1.3 Temperature dependence of mobility

(i) Scattering at phonons $\Rightarrow \propto T^{-\frac{3}{2}}$

$T < 100\text{K}$: acoustic phonon scattering dominates

T > 100K: optical — — "

(ii) Scattering at ionized impurities

Consider a non-ideal crystal at low temperatures, then the mobility decreases with decreasing T : $M \propto T^{3/2}$

II.1.4 Charge transport in disordered materials

In materials with high disorder, band theory no longer works

But there are some successful models like the Gaussian Disorder model.

Here we have a Gaussian-distribution of the DOS with standard deviation σ_{DOS}

Random hopping occurs between two non-equal states, e_i, e_j

Two assumptions were made:

- Energies of defect e^- and transport states exhibit a Gauss-dist. of DOS
 - Hopping rate is given by the Boltzmann factor

When a charge moves from one to the next molecule, the lattice movement will follow resulting in a coupling of a charge carrier and lattice vibration (phonon)
⇒ Polaron is created

Hopping transport is described by three regimes:

- Tunneling regime : At low T, the mobility exhibits a band like T-dependence
→ Coherent electron transport
 - Hopping regime : Above crit. temp. T_h , the mobility shows activation behaviour, e^- transfer processes are field-assisted and thermally activated (involve only nearest neighbours)
→ Incoherent electron transport
 - Electron scattering regime: e^- scattered at thermal phonons, decrease of mobility

Crossover from band to hopping transport:

- Weak e^- -phonon coupling: bandlike, μ dominated by coherent e^- transport, $\mu \uparrow$ for $T \downarrow$
- Med. e^- -phonon coupling: bandlike at low T , weaker T dependence at high T
- High e^- -phonon coupling: three regimes from above

II.2 Electronic structure of surfaces and interfaces

Lit: p. 35

II.2.1 Surfaces

Shockley states

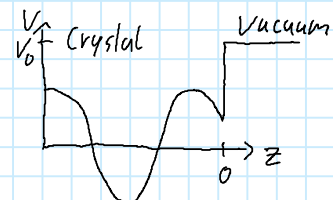
Assumption: 2D surface of an ideal crystal, e^- nearly free, bulk as semifinite chain with the surface at the end.

$$\text{The potential has the form: } V(z) = \hat{V} \left[\exp\left(\frac{2\pi i z}{a}\right) + \exp\left(-\frac{2\pi i z}{a}\right) \right] = 2\hat{V} \cos\left(\frac{2\pi i z}{a}\right)$$

at the surface ($z=0$) we have an abrupt change in V to V_0

\Rightarrow S-Eq. :

$$\left[-\frac{\hbar^2}{2m} \frac{d^2}{dz^2} + V(z) \right] \psi(z) = E \psi(z)$$



For $z \ll 0$ we can neglect surface effects and assume $V(z) = V(z+na)$

\Rightarrow Solution are Bloch waves (2.29)

Near the surface ($z=0$) the solution has to fulfill:

- Boundary cond. $E_{\text{vac}} = V_0 = \text{const}$ for $z > 0$
- Has to solve the S-Eq. for $z < 0$
- Both solutions have to match at $z=0$ (ψ and $\frac{\partial \psi}{\partial z}$)

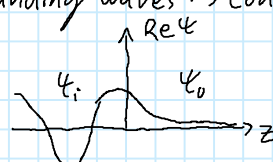
At $z > 0$: Exponential decay

$$\psi_0 = D \exp\left[-\sqrt{\frac{2m}{\hbar^2}(V_0 - E)} z\right] \quad \text{with } E < V_0$$

Solutions of $z < 0$ and $z > 0$ can only match for standing waves \Rightarrow Condition:

$$\psi_0(z=0) = \alpha \psi_i(z=0, \kappa) + \beta \psi_i(z=0, -\kappa)$$

Possible solution: Bloch



If we allow complex wavevectors $\kappa = -iq \Rightarrow$ More solutions possible, but with same characteristics

Resulting states are the so called surface states

The matching conditions are leading to two effects:

- e^- in these states are localized within a few Å of the surface plane
- Allowed energy states are restricted + energy of surface state lies within the energy gap of the crystal

Surface states of ideal clean surfaces are called Shockley-states

Tamm states:

Starting point:

tightly bound electrons and the emergence of bands is explained by WF overlap of neighboring atoms in the bulk.

Then surface states are understood by the ex. of dangling bonds at the surface (absence of a bounding partner)

Splitting and shifting of energy levels is smaller than in the bulk

Greater disturbance by surface \rightarrow larger deviation of energy of surface states from the bulk states

Energetically higher/lower laying surface states have CB/VB character

SC is neutral when all CB states are empty and all VB states are occupied. These states have charging character:

- Acceptor-like states are neutral when unoccupied, negatively charged when occupied
- Donor-like: positively when unoccupied, neutral when occupied

Other surface states:

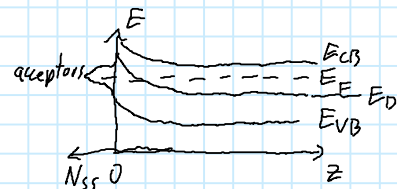
Extrinsic:

- Missing surface atoms act as traps for charge carriers

Space charge layers at SC surfaces, band bending

Placing a single charge into locally neutral e^- plasma leads to a rearrangement of the neighbourhood \rightarrow Screening such that the \vec{E} -field vanishes

- Metals: $n_e \approx 10^{22} \text{ cm}^{-3}$, screening length $\sim \text{\AA}$
- SC: $n_e \approx 10^{17} \text{ cm}^{-3}$, screening length $\sim 100 \text{ \AA}$



Surface state may carry charge, screened by charge inside the SC

\Rightarrow Charge neutrality: $Q_{ss} = -Q_{sc}$

\Rightarrow Band bending

Three types of band bending:

- Depletion:

Three types of band bending:

- Depletion:

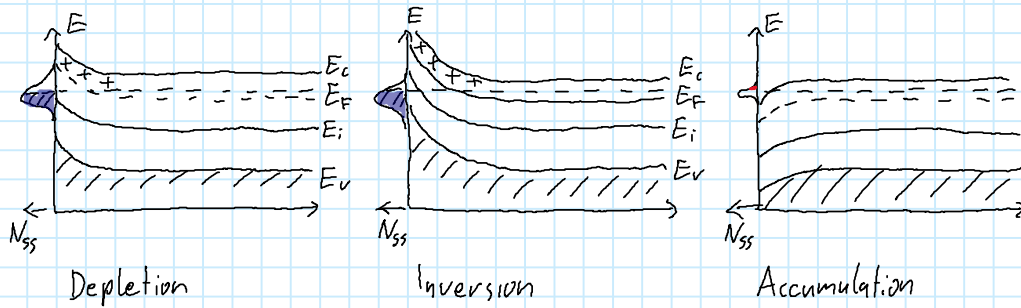
Band bending \rightarrow Free CB e^- 's pushed away from surface \rightarrow Density lowered
(In n-type SC: Decrease of free e^- , increase of holes)

- Inversion layer:

Higher densities N_{ss} of surface states at low energies \rightarrow stronger upward bending

- Accumulation layer:

Surface states at higher energies, partially empty & positive surface charge
 \rightarrow Compensated by negative space charge \rightarrow downward bending



Quantitative description

Maxwell-eq.: $\text{div } E = \frac{\sigma(x)}{\epsilon \epsilon_0}$ with σ (space charge density) + $E = -\nabla \phi$

$$\Rightarrow \boxed{\frac{d^2 \phi(x)}{dx^2} = -\frac{\sigma(x)}{\epsilon \epsilon_0}} \quad \text{Poisson eqn. with } 0 < x < \infty$$

$$\sigma(x) = e [N_d^+(x) - N_a^-(x) + p(x) - n(x)]$$

II. 2.2 Metal-metal interface

Two metals with work functions $e\phi_1, e\phi_2$ in contact: $M_1=M_2, E_{F_1}=E_{F_2}$



e^- from metal with low work function flows to metal with higher \rightarrow leading to a dipole layer

II. 2.3 Metal-SC interface

E_F 's align, dependent on work function $e\phi$ and e^- affinity of SC π three scenarios can occur

1. Schottky barrier: High work function, n-type SC

- e^- from SC to metal
- Depletion region forms
- Upward band bending

- Depletion region forms
- Upward band bending
- Positive space charge of ionized donors

Max band bending, bc. e^- has to overcome from metal to CB of SC

$$e\phi_{SB} = e\phi_m - \chi_{SC} \quad \text{Schottky barrier}$$

$$\text{Energy of bulk } e^- : eV_B = e\phi_m - \chi_{SC} - (E_{CB} - E_F)$$

2. Ohmic contacts: Low work function, n-type SC

- e^- from metal \rightarrow SC
- Accumulation / Inversion region
- Downward band bending
- Negative space charge of ionized acceptors

$$U = R \cdot I$$

metal - p-type SC analogously

3. Rectifying behavior: Schottky barrier under ext. voltage

(i) No ext. Voltage $U=0$

e^- in SC need to be thermally activated to overcome barrier \Rightarrow thermionic emission current

Compensated by e^- current from metal \rightarrow SC

\Rightarrow In total: $I=0$

(ii) $U > 0$

In SC $E_F \uparrow$

\Rightarrow barrier reduces

Number of e^- in CB obey Boltzmann-statistics $\Rightarrow I(U) = I_0 \left[\exp\left(\frac{eU}{k_B T}\right) - 1 \right]$

$\lceil I_0$ depends on assumptions, e.g. thermionic emission, diffusion, ... \rfloor

(iii) $U < 0$

In SC $E_F \downarrow$

\Rightarrow Barrier height raises \Rightarrow Only current from metal to SC observed

\lceil For $U < 0$, current only depends on Schottky barrier height \rfloor

! e^- from metal \rightarrow SC: see Schottky barrier $e\phi_{SB}$
 $SC \rightarrow$ metal: only band bending eV_{eq}

II. 2.4 SL-SC interface, pn-junction

Two important lengthscales:

Two important lengthscales:

- Interface dipoles due to flow of charges across the interface
- Space charge layers \rightarrow band bending $\sim 100 \text{ \AA}$ into bulk due to lower charge carrier density

Important effects:

- Energy level alignment, related to band offset ΔE (diff. of $E_{VB,\max}$ & $E_{CB,\min}$)
- Band bending (result of E_F alignment in thermal equilibrium)
Can be described as before + junction is current free in therm. equ. + doping determines pos. of E_F

I-V-characteristics

Assumptions: (i) Density of donors N_D (n-side) & acceptors N_A (p-side) is const.

(ii) All dopants are ionized: $N_D = N_D^+$; $N_A = N_A^-$

Contact of SC's:

holes from p-side to n-side

e^- from n-side to p-side

+ Formation of space-charge region (depletion region) at interface

Concept of majority charge carriers

holes diffuse to n-side recombining with majority charge carriers (e^- on n-side)

e^- p-side (holes on p-side)

\Rightarrow Quasi-neutral region on both sides of space charge region at the interface

\Rightarrow Diffusion current I_r (recombination current)

Spatial extend of space charge region is defined by Debye screening length L_D

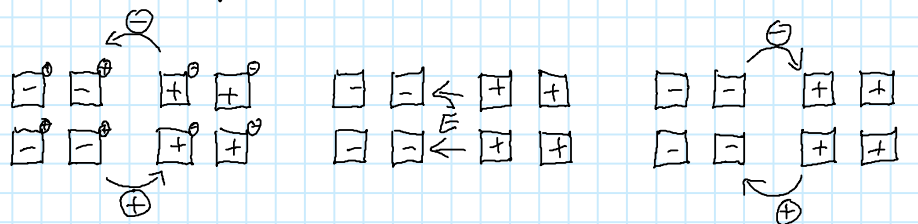
$$L_D = \sqrt{\frac{2\epsilon\epsilon_0\psi_s}{\rho_0}} \propto \frac{1}{\sqrt{\rho_0}}$$

with $\psi_s = \phi_{surf} - \phi_{bulk}$ pot. diff
 ρ_0 : space charge density

Space charge regions \rightarrow \vec{E} -field \rightarrow thermally generated minority charge carrier counteracting

\Rightarrow generation current I_g

No ext. voltage: $I_v(0) + I_g(0) = 0$



Majority carrier flow

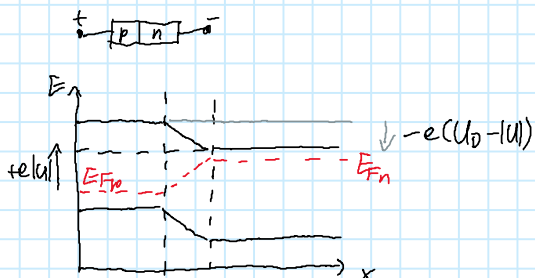
Resulting \vec{E} -field

minority carrier flow

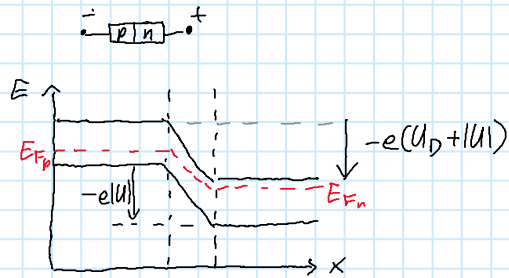
Width of space charge region based on Poisson-equ. + transition between p- and n-region is abrupt:

$$w = \sqrt{\frac{2\epsilon_0}{e} \frac{N_A + N_D \cdot U_D}{N_A N_D}} \text{ with } U_D = eV_B \text{ ch. static pot. at interface (built-in pot.)}$$

$U > 0$: Passband (Durchlassbereich)



$U < 0$: "Sperrung"



Current-Voltage characteristics of a pn-junction

$U = 0$:

Recombination & generation current are cancelling each other out

$I = 0$

$U > 0$ (p-side):

Pot. barrier reduced by $-e(U_D - |U|)$

Recombination current: $I_{nr}(U) = I_{nr}(0) \exp\left(\frac{eU}{k_B T}\right)$; $I_{pr}(U) = I_{pr}(0) \exp\left(\frac{eU}{k_B T}\right)$

Generation current: independent of barrier

$$\Rightarrow I_{tot}(U) = (I_{nr}(0) + I_{pr}(0)) \left[\exp\left(\frac{eU}{k_B T}\right) - 1 \right]$$

$U < 0$ on p-side:

Pot. barrier reduced by $-e(U_D + |U|)$

Generation current dominates and reaches $-(I_{nr}(0) + I_{pr}(0))$ for large $|U|$ (saturation current)

II.3 Devices: Photovoltaic cells, light emitting diodes and field-effect transistors

Lit.: p. 52

II.3.1 Solar cells

Principle: Absorption of a photon with $h\nu > E_g$

Working principle

(i) Absorption of light and creation of e^- -hole pairs

γ absorbed $\rightarrow e^-$ from VB to CB \rightarrow hole left $\rightarrow e^-$ + hole = exciton \rightarrow free charge carrier

Generation rate of e^- -hole pairs:

$$G = (1 - s) \int_{\lambda_{min}}^{\lambda_{max}} (1 - r(\lambda)) f(\lambda) e^{-\alpha(\lambda)} \alpha(\lambda) d\lambda$$

$\begin{matrix} \text{reflectance} \\ \text{L}_{\text{G,rd}} \\ \text{L}_{\text{flux}} \\ \text{shadowing} \end{matrix}$ $\begin{matrix} \text{L}_{\text{abs,coeff}} \\ \text{L}_{\text{abs}} \end{matrix}$

$$L_{\text{Grid}}^{\lambda} \quad L_{\text{flux}} \quad L_{\text{abs. coeff}}$$

shadowing
factor

(ii) Separation of e^- -hole pairs, carrier transport

E -Field due to built-in pot. $\rightarrow e^-$ -holes separated \rightarrow free charge carrier diffuse to electrodes

Current density dom. by minority charge carrier:

$$\vec{\nabla} \vec{j}_n = q \left(-G + R_n + \frac{\partial n}{\partial t} \right) ; \vec{\nabla} \vec{j}_p = q \left(G - R_p - \frac{\partial p}{\partial t} \right)$$

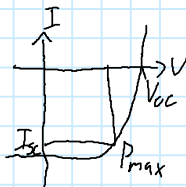
(iii) Loss mechanism: Recombination

- Via trap states
- Radiative recomb.
- Auger recomb. + Excitation energy \rightarrow to another charge carrier
- Via surface states

I-V-characteristics, figures of merit

Parameters: Open circuit volt. V_{oc} ; short circuit I_{sc} ; Max. power point $V_{mp}, I_{mp} = \max$

• Fill factor: $FF = \frac{V_{mp} I_{mp}}{V_{oc} I_{sc}}$



• Power conversion eff.: $\eta = \frac{P_{mp}}{P_{in}}$ (P_{in} from solar spec.)

• Ext. collection eff.: $\eta_c^{ext} = \frac{I_{sc}}{I_{inc}}$ \leftarrow max. possible photocurrent of area A with $E > E_g$

• Internal collection eff.: $\eta_c^{int} = \frac{I_{sc}}{I_{gen}}$ \leftarrow light gen. current

Theoretical efficiency limit (Shockley Queisser limit)

Direct E_g / e^- -hole-pairs with $h\nu_{th} = \Delta E_{th} / \text{solar spectrum} = bb$ -spectrum

In - vs. Organic solar cells

- $E_0 < E_1$
- In organic: pn-junction not by doping but with two o. SC's
- Collection eff. lower
- + lower process T, absorption can be tuned to solar spectrum

II. 3.2 LEDs

Working principle

Solar cells



Tot. carrier density: $n = n_0 + \Delta n$, $p = p_0 + \Delta p$

Equilibrium Excess due to injection

Recomb. rate: $R = -\frac{dn}{dt} = -\frac{dp}{dt} = B np$

L recomb. coeff.

$\Delta n(t) = \Delta p(t)$ (recomb. in pairs)

Electrical characteristics of LEDs

Charge in depletion area due to stationary ionized donors & acceptors, produces built-in potential

\Rightarrow Diffusion voltage $V_D = \frac{k_B T}{e} \ln \left(\frac{N_A N_D}{n_i^2} \right)$ with N_A, N_D concentrations

Current-voltage characteristics

Shockley equation:

$$I = e A \left(\sqrt{\frac{D_p}{\tau_p}} \frac{n_i^2}{N_D} + \sqrt{\frac{D_n}{\tau_n}} \frac{n_i^2}{N_A} \right) (e^{eV/k_B T} - 1)$$

with A : area; $D_{n/p}$, $\tau_{n/p}$: Carrier diffusion const. / Lifetimes

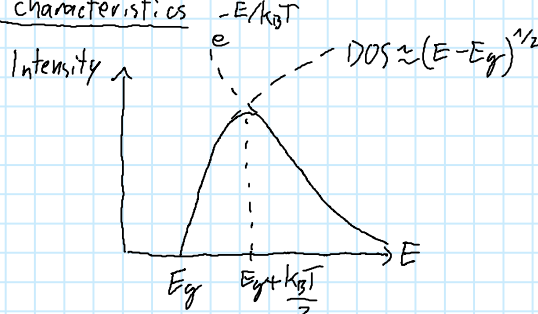
V : external voltage

$V \gg k_B T$: All dopants ionized:

$$I = e A \left(\sqrt{\frac{D_p}{\tau_p}} N_A + \sqrt{\frac{D_n}{\tau_n}} N_D \right) (e^{(V-V_D)/k_B T})$$

Current \uparrow for $V \rightarrow V_D \Rightarrow$ Definition of thresh voltage $V_{th} \approx V_D \approx E_g/e$ "drive voltage"

Emission characteristics



Emission distinguished by bandgap:

direct: Momentum of e^- and hole must be equal

indirect: \downarrow + phonon

In general: emission density: $I(E) \propto \underbrace{(E - E_g)^{1/2}}_{\text{DOS of } e^- \text{ and holes of same momentum}} e^{-E/k_B T}$

DOS of e^- and holes of same momentum

$$\text{Max. emission: } E = E_g + \frac{1}{2} k_B T$$

Band width (below) $\Delta E = 1.8 k_B T$

Efficiencies

- Internal quantum eff. $\eta_{int} = P_{int}/h\nu$ "emitted photons/s"

Efficiencies

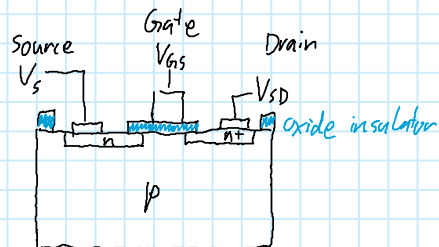
- Internal quantum eff. $\eta_{int} = \frac{P_{int}/h\nu}{I/e}$ " $\frac{\# \text{emitted } \gamma\text{'s/s}}{\# \text{injected } e^-/\text{s}}$ "
- Extraction eff.: $\eta_{extract} = \frac{P/h\nu}{P_{int}/h\nu}$ " $\frac{\# \gamma\text{'s emitted in free space/s}}{\# \gamma\text{'s emitted from active region/s}}$ "
- External quantum eff.: $\eta_{ext} = \frac{P/h\nu}{I/e} = \eta_{extract} \cdot \eta_{int}$
- Power eff.: $\eta_{power} = \frac{P}{IV}$

2.3.3 Field effect transistors

Base of electronic devices, mostly used MOSFET

Different types:

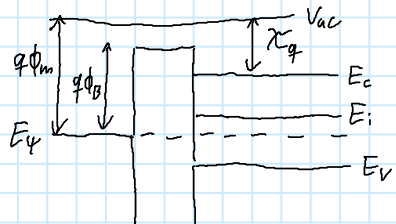
- self-conducting / self locking
- e^- / hole conduction



Band structure

Assumption: $V_{DS} \rightarrow 0$ (linear response regime)

+ few or no surface states; flat band in absence of V_{GSS}



$q\phi_m$: Work function

X_q : e^- -affinity, moving e^- from vac to CB

E_i : Intrinsic Fermi energy

(same distance to $E_{i,max}$ & to $E_{i,min}$)

$q\phi_B$: Barrier height of oxide insulator

Applying a gate voltage

$V_{GSS} < 0V \Rightarrow$ Chemical pot. of metal ↑

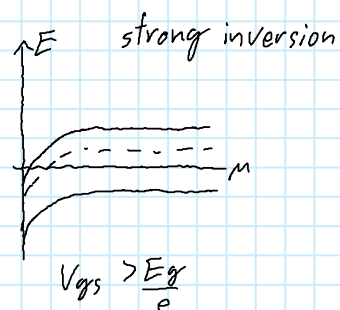
⇒ band bending and accumulation of charge (holes)

$V_{GSS} \geq 0V$

⇒ Depletion ($\# \text{holes} \downarrow$ but $\# e^- \rightarrow$)

⇒ Weak inversion, intrinsic EF below chem. pot.

⇒ Strong inversion, E_{CB} below chem. pot.



Calculation of band structure in a MOSFET

Additional position-dependent pot. $\psi(x)$

$$\Rightarrow E_{CIV} = E_{CIV}(\infty) + \psi(x)$$

⇒ $n_c(x), p_v(x)$ with bulk concentration N_{C0}, P_{V0}

$$n_c(x) = N_{C0} e^{-\epsilon\psi/k_B T}, p_v(x) = P_{V0} e^{-\epsilon\psi/k_B T}$$

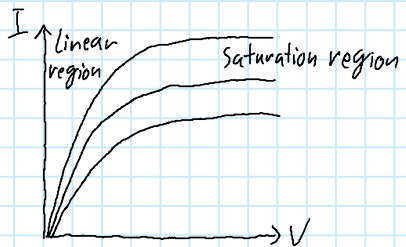
For V_s (surface potential / "gate voltage") one needs to solve the Poisson-equation:

$$\frac{d^2\psi}{dx^2} = -\frac{\sigma(x)}{\epsilon_r \epsilon_0} \quad \text{where } \sigma(x) = q(N_D^+ - N_A^- + p_v - n_c)$$

With boundary conditions $\sigma(x)=0$, $\psi(x)=0$, $x \rightarrow \infty$ (bulk), $(N_D^+ - N_A^- = N_{co} - P_{vo})$

+ the field strength $F = -\frac{\partial \psi}{\partial x} \Rightarrow \left(-\frac{\partial \psi}{\partial x}\right)^2 = ..$

Current-voltage-characteristics



Zusammenfassung Chapter01 and 02 b

Mittwoch, 13. Juli 2022 18:35

2.4 Electronic properties of systems with reduced dimensions

Lit.: 74

Recap:

$$\bar{e}^- \text{ density in Fermi sphere: } n = \frac{N}{V} = \frac{k_F^3}{3\pi^2}$$

$$\text{DOS: } g(\epsilon) = \frac{1}{V} \frac{\partial N}{\partial \epsilon} = \frac{\partial n}{\partial \epsilon}$$

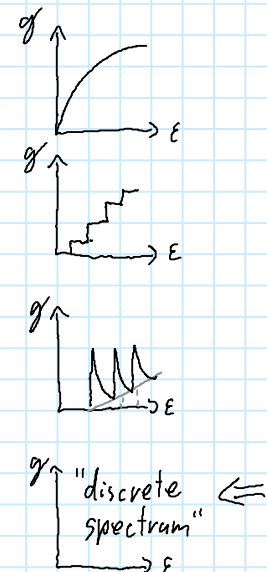
In different dimensions with eff. mass m^*

$$3D: \quad g(\epsilon) = \frac{\sqrt{2\epsilon m^3}}{\pi^2 \hbar^3} \propto \sqrt{\epsilon}$$

$$2D: \quad = \frac{m^*}{\pi \hbar^2} \propto \text{const.}$$

$$1D: \quad = \frac{1}{\pi \hbar} \sqrt{\frac{2m^*}{\epsilon}} \propto \frac{1}{\sqrt{\epsilon}}$$

$$0D: \quad = \delta(\epsilon)$$



2.4.1 (Quasi-) 2d quantization in heterostructures

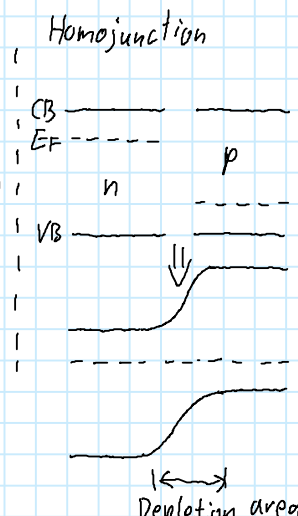
Two different junctions:

- Homojunction:

Interface between two SC's with identical E_g (may have diff. doping)

- Heterojunction:

Diff E_g

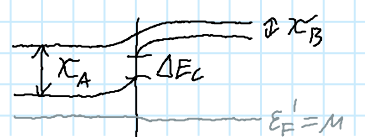


Heterojunction leads to a chem. pot. through the whole material $\Rightarrow E_{F_1}' = E_{F_2}' = \mu$ V/r

In equilibrium for both junctions:

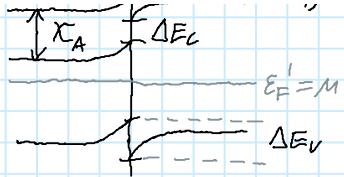
- Depletion regions
- Band-bending
- Creation of a built-in potential $\Phi_{bi}(r)$

+ in hot carrier scattering band edge discontinuity ΔE , $\Delta \sigma$



Creation of a band bending potential at $V_{bi}(r)$

+ in heterojunctions: band edge discontinuities $\Delta E_C, \Delta E_V$



Example: p. 76

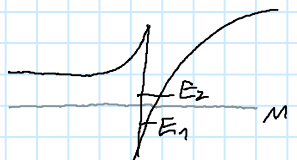
Combination leads to "self-consistent" CB structure

\Rightarrow Creation of triangular quantum well at interface

By tuning \rightarrow only 1st discrete energy level below E_F

\Rightarrow 2D-e⁻-gas

\Rightarrow Electrostatics (Poisson); QM(SG); triangular pot. well can be solved



- Lowest quantized state can be related to F:

$$E_1 = \left(\frac{\hbar^2}{2m^*} \right)^{1/3} \left(\frac{9\pi e F}{8} \right)^{2/3}$$

- Surface density of e⁻; where band bending occurs

$$F = \frac{N_s e}{\epsilon_0 \epsilon_r} \Rightarrow E_1 = \text{const.} \cdot N_s^{2/3}$$

- N_s also related to E_F & k_F

$$E_F = E_1 + \frac{\hbar^2 k_F^2}{2m^*} = E_1 + \frac{\pi \hbar^2}{m^*} N_s \quad \text{with} \quad \text{2D: } k_F^2 = 2\pi N_s ; \text{ 3D: } k_F^3 = 3\pi^2 N_s$$

Assuming const. dopand density N_d & charge neutrality $N_d w = N_s$ (along depletion length w)

$$\Rightarrow V_{dep} = - \int_0^{-w} F dz = \frac{e N_d w^2}{2 \epsilon_0 \epsilon_r}$$

$$\Rightarrow \Delta E_v = E_1(N_s) + \frac{\pi \hbar^2 N_s}{m^*} + \epsilon_0 + eV_{dep} \quad \text{L Spacing between } E_F \& E_C$$

2.4.2 Conductance in low-dimensional systems

Return to BTE density of VB e⁻

$$\vec{j} = -ne\vec{v} = -\frac{ne\vec{p}}{m^*}$$

$$\Rightarrow \frac{d\vec{p}}{dt} = -\frac{\vec{p}(t)}{\tau} + \vec{f}(t) \quad \vec{f}: \text{external field}$$

Case $\vec{f}(t) = -e\vec{E}$

$$\Rightarrow \frac{d\vec{p}}{dt} = -\frac{\langle \vec{p} \rangle}{\tau} - e\vec{E} = 0 \Rightarrow \langle \vec{p} \rangle = \underbrace{\frac{ne^2 \tau}{m^*}}_{= \sigma} \vec{E}$$

= or "Boltzmann conductivity"

Role of e⁻ at Fermi surface

For low fields, the electronic transport can be regarded as a property of e⁻ at Fermi surface

For low fields, the electronic transport can be regarded as a property of e^- at Fermi surface with $\frac{\Delta k}{k_F} \ll 1 \Rightarrow \frac{\Delta \vec{p}}{\hbar k_F} \ll 1 \vee \frac{eE\tau}{\hbar k_F} \ll 1 \Rightarrow E < 10^5 \text{ V m}^{-1}$

At low T ($E \rightarrow 0$): linear response properties thus the perturbations of Fermi sphere is minimal

$$\text{Free } e^-: \varepsilon_F = \frac{\hbar^2 k_F^2}{2m} \text{ with } n = \frac{k_F^d}{d \cdot \pi^{d-1}}, d \in \{2, 3\}$$

$$\Rightarrow \text{DOS} S: g(\varepsilon_F) = \left. \frac{dn}{d\varepsilon} \right|_{\varepsilon=\varepsilon_F} = \frac{2m(2m\varepsilon)^{\frac{d}{2}-1}}{\hbar^d \cdot 2 \pi^{d-1}}$$

$$\Rightarrow \sigma_B = g(\varepsilon_F) e^2 \cdot \underbrace{\frac{2\varepsilon_F \gamma}{md}}_{D} = g(\varepsilon) e^2 D + \text{quantum corrections}$$

$$D = \frac{v_F^2 \gamma}{d} \quad \text{"Einstein diffusion constant" with } v_F = \frac{\hbar k_F}{m}$$

Length scales:

- $\lambda_F = \frac{2\pi}{k_F}$

- Elastic mean free path / elastic scattering or mom. relaxation length

$$l_e = v_F \tau_e, \tau_e \text{ elastic sat. time}$$

- Inel. scat. length: $l_{in} = \sqrt{D \tau_{in}}$ Energy relax./phase relax. of e^- wave function

- Phase coherence length $l_\phi = l_{in}$ (sometimes)

- Magnetic length $l_B = \sqrt{\frac{\hbar}{eB}}$

- Sample size L_x, L_y, L_z

Z. 4.3 Low-dim. systems in high magnetic fields

Landau quantization

$$H\psi = \frac{1}{2m} (\vec{p} - e\vec{A})^2 \psi = E\psi$$

Leading to energy levels in x-y plane

Number of states per level: boundary condition $\psi(y) = \psi(L_y + y)$ with $k_y L_y = 2\pi n$, e^- within the sample $0 \leq x \leq L_x$

$$\Rightarrow 0 \leq \frac{\hbar k_y}{eB} \leq L_x \Rightarrow 0 \leq n \frac{2\pi \hbar}{eB} \leq L_x L_y$$

$$\Rightarrow n_{\max} = \frac{eB}{2\pi \hbar} L_x L_y \quad !\text{Without Spin 2!}$$

$\Rightarrow g(\varepsilon)$ splits up to discrete energy levels with spacing of two

Filling factor (occupied Landau levels + partially upper level):

$$n = n_{2n} - n_{2n-1}$$

Filling factor (occupied Landau levels + partially upper level):

$$v = \frac{n_{2D}}{eB/2\pi\hbar} = \frac{n_{2D}\hbar}{eB}$$

Shubnikov de Haas effect

Longitudinal resistance ρ_L or conductance $\sigma_L = (\rho_L)^{-1}$ exhibits oscillations in a quantized field that fulfills $w_c \tau > 1$ and $T \ll k_B T$

↳ several cyclotron orbits

⇒ Oscillation period changes with $\Delta(1/B)$

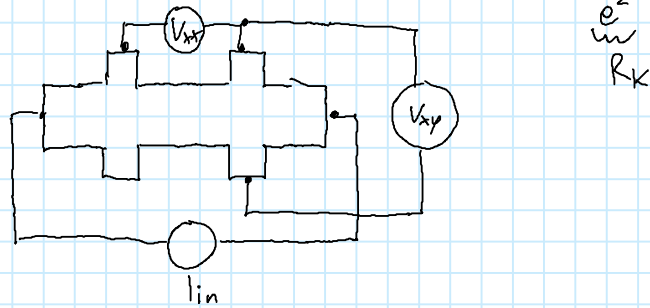
⇒ Carrier concentration $n_e \approx \frac{e}{h} \frac{1}{\Delta(1/B)}$



Quantum Hall effect

Nearly zero resistance in longitudinal direction: $\rho_L \approx 0 - 10^{-10} \Omega \square$

constant plateaus in transversal direction: $\rho_T \approx \frac{h}{e^2} \frac{1}{n} = \frac{1}{n} 25812.807 \Omega$, $n \in \mathbb{N}$

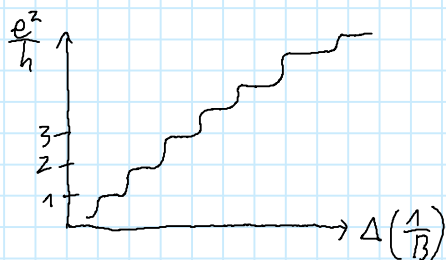


"Skipping" cyclotron orbits that are reflected at the edges → net transport of e^-

char. distance of edge states $\approx D_{ch} = \sqrt{(2\nu+1) \frac{\hbar}{eB}}$

Simultaneous zeros in ρ_L & ρ_T $\Leftrightarrow E_F$ does not coincide with Landau levels

Max. of ρ_L & change in plateau $\Leftrightarrow E_F$ does " "



Multiple integers of $\frac{2e^2}{h}$ for low fields

$\frac{e^2}{h}$ for high fields

Fractional Quantum Hall effect

Comparable to QHE

Plateaus at fractional multiples of $\frac{h}{e^2}$: $\rho_L \approx 0$ & $\rho_T = \frac{h}{e^2} \frac{p}{q}$; $p, q \in \mathbb{N}$

Reason: Composite fermions (def. # of e^- + flux quanta)

Eff. magn. field: $\vec{B}'^\pm = \vec{B} \pm 2pn\phi_0$ with n : 2D particle density, $2p$ # vortices in comp. fermion

Reason: composite fermions (det. # of e^- + flux quanta)

Eff. magn. field: $\vec{B}^* = \vec{B} \pm 2pn\phi_0$ with n : 2D particle density, $2p$ # vortices in comp. fermion and $\phi_0 = \frac{\hbar}{e}$ composite fermion flux quantum

Graphene Spoiler:

QHE in graphene

single layer graphene has quantisation of $\frac{4e^2}{h}$

2.4.4 (Quasi-) 1 dim. systems: quantum wires

When motion of e^- is constrained, width of channel $\sim \lambda_F$

(Again) three regimes

- Ballistic regime: $l_\phi \gg l_e \gg L, W$

Motion of charge carriers dom. by geometry of the wire



- Quasi-ballistic regimes: $l_\phi \gg L \gg l_e, W$

small, finite scattering centres are dom., $\Gamma < \Delta g \ll \frac{e^2}{\pi \hbar}$



- Diffusive regime: $l_\phi \gg L, W > l_e$

only exists, when many modes are occupied



Creation:

2D e^- gas, quantum point contacts have tunable widths

Pair of contacts separated by a narrow gap / "split-gate" on top of 2D- e^- gas

Negative voltage in electrodes $\rightarrow e^-$ gas below electrodes is depleted + potential wall

\rightarrow No e^- transport in this areas

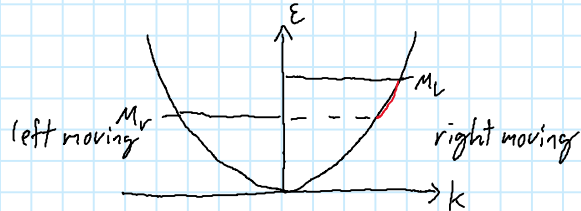
\Rightarrow 1D channel

Conductance & transmission in mesoscopic systems

Assume ballistic conductor

\Rightarrow No scattering \Rightarrow Current = 1d channel of \approx free e^- [$m=m^*$]

But parabolic dispersion $\epsilon(k) = \frac{\hbar^2 k^2}{2m^*}$



Right-moving states from chem. pot M_L

$\Rightarrow V_0$ (large diff.) $-e\Delta V = M_L - M_R$

$$\Rightarrow I = - \int_{M_R}^{M_L} g_{1D}(\epsilon) eV(\epsilon) d\epsilon$$

$$g(\epsilon) = g(k) \frac{\partial k}{\partial \epsilon} = \frac{1}{\pi} \frac{dk}{d\epsilon}$$

L velocity of states $v(\epsilon) = \frac{\hbar k}{m^*} = \frac{1}{\hbar} \left(\frac{\partial \epsilon}{\partial k} \right)$

$$\Rightarrow I = \frac{e^2}{\pi \hbar} \Delta V \Rightarrow \text{Conductance } G = \frac{I}{\Delta V} = \frac{2e^2}{h} \quad (2 \cdot \text{from spin})$$

Quantization of G

This formalism can be described by the four-terminal Landauer-Büttiker formula:

$$\frac{h}{2e} I_i = (N_i - R_{ii}) M_i - \sum_{j \neq i} T_{ij} M_j$$

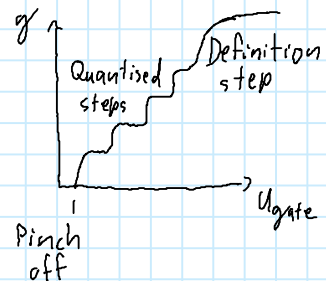
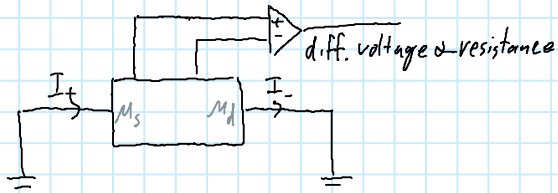
I_i : current into contact

N_i : # channels involved in transmission

R_{ii} : # reflected channels

T_{ij} : # transmitted channels ($j \rightarrow i$)

M_i : appropriate chem. pot. of channels



(analogous to QHE with magn. field)

For quantum point contact (QPC) with def. small # of perf. trans. subbands

N_N & $N_V \ll N_w$ ($\hat{=}$ # channels in the wide region)

$$\Rightarrow \frac{h}{2e} I = (N_w - (N_w - N_N)) M_S - N_N M_D = N_N (M_S - M_D)$$

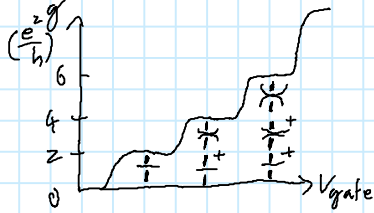
$$\Rightarrow \frac{eI}{M_S - M_D} = G = \frac{2e^2}{h} N_N \quad \text{Conductance quantisation in 1D channels is recovered}$$

• Transport measurements in linear regimes (small source-drain-voltage V_{sd}
 $\rightarrow M_R \ll \epsilon \ll M_L$)

• $V_{varo.} \uparrow \Rightarrow$ 2D e gas def. 1D constriction, at $V_{varo.} \rightarrow$ def. step as drop of conductance

$$\rightarrow M_r < \epsilon < M_L$$

- $V_{\text{gate}} \uparrow \Rightarrow 2D e^-$ gas def. 1D constriction, at $V_{\text{gate},\text{crit}}$ \rightarrow def. step as drop of conductance
 \Rightarrow Discrete 1D subbands evolve



- After last mode depleted \rightarrow "Pinch off", (conductance $\rightarrow 0$)
- Steps of $\frac{e^2}{h}$, for magn. field $\frac{e^2}{h}$

Nonlinear regime:

$V_{\text{sd}} \uparrow \Rightarrow$ transport window $M_L - M_r \uparrow$

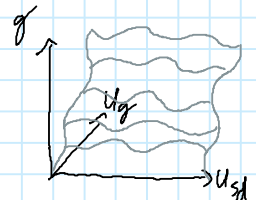
\nexists left- and right moving states can differ $\sim V_{\text{sd}}$

\Rightarrow odd diff. of left & right \Rightarrow plateaus at odd multiples of $\frac{e^2}{h}$

even — —

" — —

even — —



2.4.5 (Quasi-) 1dim systems: quantum dots (QD)

- Colloidal quantum dots:

- Preparation via wet chemistry or nanocrystal prep. by chem. vapour deposition

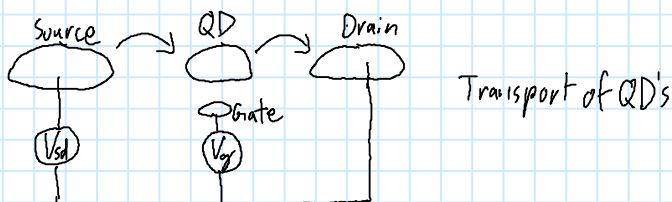
- Epitaxial quantum dots:

Due to stress/strain depending on slightly mismatch of lattice const.

\Rightarrow self-assembled QD's during epitaxial growth

- Electrostatically induced QD's

By split gates



e^- can tunnel from source to QD when states are available
 tunnel QD to drain

- Discrete energy level sys. can be shifted cont. by V_g

- $M_s - M_d$ is identified with V_{sd}

- Depending on energys of Source, QD, Drain, transport can either be blocked (Coulomb blockade) or allowed

- energy gap between available states $\approx \frac{e^2}{C_\Sigma}$, C_Σ : sum of capacitances between S, QD, D

... Coulomb blockade ... f ... Landauer transport ...

- energy gap between available states $\approx \frac{e}{C_{\Sigma}}$, C_{Σ} = sum of capacitances between D, X, Y, D
- Charge quantisation in form of single e^- transport
- Coulomb blockade oscillations in linear regime (small V_{sd})
 - ↳ no level or single level with $M_d \leq E \leq M_s$
- Non linear regime:
 - gate regions with blocked transport \downarrow with $V_{sd} \uparrow$
 - \Rightarrow Coulomb diamonds where the conductance = 0
 - with $V_{sd} \uparrow \uparrow \Rightarrow$ several energy levels with $M_d \leq E_n < E_{n+1} < \dots < M_s$
 - \Rightarrow \uparrow values of conductance

Outlook

- QD's can act as bright emitters
- λ def. by optical E_g
- Single photon emission

Zusammenfassung Chapter03

Sonntag, 17. Juli 2022 14:24

3. Optical properties of nanostructure

Lit.: p. 103

3.1 Plasmonics

Plasmonics: Interactions between e.m. waves & metal interfaces

M. equations:

$$\nabla \cdot \vec{D} = \rho$$

$$\nabla \cdot \vec{B} = 0$$

$$\nabla \times \vec{E} = - \frac{\partial \vec{B}}{\partial t} \quad ! \text{ hier } F$$

$$\nabla \times \vec{H} = \vec{j} + \frac{\partial \vec{D}}{\partial t}$$

Limit of linear, isotropic & non-magnetic:

$$\vec{D} = \epsilon_0 \epsilon \vec{E}$$

$$\vec{B} = \mu_0 \vec{H}$$

With Dielectric function $\epsilon(\omega) = \epsilon' + i\epsilon''$

Connected to compl. index of refraction: $n_c(\omega) = n + i\kappa = \sqrt{\epsilon}$

$$\Leftrightarrow \epsilon' = n^2 - \kappa^2, \epsilon'' = 2n\kappa \quad | \quad n^2 = \frac{\epsilon'}{2} + \frac{1}{2} \sqrt{\epsilon'^2 + \epsilon''^2}, \kappa = \frac{\epsilon''}{2n}$$

$n(\omega)$: Dispersion

$\kappa(\omega)$: Absorption

Beer's law: Intensity of a light beam in a medium: $I(x) = I_0 e^{-\alpha x}$

$$\text{with } \alpha(\omega) = \frac{2\kappa(\omega)}{c}$$

3.2 Bulk plasmons

Plasma model: e^- gas with density N

e^- excited to form oscillation in presence of $\vec{E}(t) = \vec{E}_0 \exp(-i\omega t)$

damped by collisions with char. rate $\gamma = \frac{1}{\tau}$

\Rightarrow Equation of motion $m\ddot{x} + m\gamma\dot{x} = -e\vec{E}(t)$ with solution $\vec{x}(t) = \frac{e}{m(\omega^2 + i\gamma\omega)} \vec{E}(t)$

e^- displaced rel. to atom core \Rightarrow Polarisation $\vec{P} = -Ne\vec{x}$

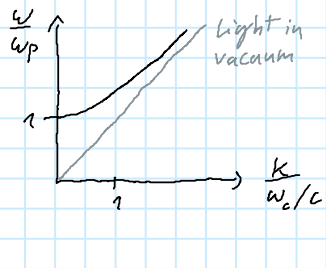
$$\Rightarrow \vec{D} = \epsilon_0 \vec{E} + \vec{P} = \epsilon_0 \epsilon \vec{E} = \epsilon_0 \left(1 - \frac{\omega_p^2}{\omega^2 + i\gamma\omega} \right) \vec{E} \quad \text{with } \omega_p^2 = \frac{Ne^2}{\epsilon_0 m} \text{ "plasma frequency"} \\ \underbrace{\epsilon(\omega)}_{\epsilon(\omega)} = 1 - \frac{\omega_p^2 \gamma^2}{\omega^2 \gamma^2 + i\omega \gamma}$$

With el. static screening $\rightarrow \epsilon(\omega) = \epsilon_{\infty} - \frac{\omega_p^2}{\omega^2 + i\gamma\omega}$
 const.

$\omega_p \ll 1$: $\alpha = \sqrt{\frac{2\omega_p^2 \omega}{\omega}}$ metals are strongly absorbing

Penetration depth into metal: $s = \frac{1}{\alpha}$ "skin depth"

$\omega_p \gg 1$: From $k^2 = |\vec{k}|^2 = \frac{\epsilon \omega^2}{c^2} \Rightarrow \omega(k) = \sqrt{\omega_p^2 + k^2 c^2}$



$\omega = \omega_p$, where for low damping $\epsilon(\omega_p) \approx 0$: collective longitudinal excitation mode

with depolarizing field $\vec{E} = -\frac{\vec{P}}{\epsilon_0}$

- Physical interpretation: collective oscillation

\rightarrow Quanta of this charge oscillation is called "Plasmons" / "bulk plasmons"

- Bulk plasmons cannot couple to transversal e.m.-fields (bc. longitudinal)

- For most metals $\omega_p \sim \text{UV}$

3.3 Surface plasmons

(Surface plasmon polaritons, SPPs)

em-excitations \sim charge density oscillations along the interface between metal & dielectric medium

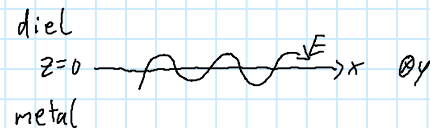
• separate M. equ. to x-y-plane extended infinitely, interface at $z=0$

\Rightarrow Conditions of continuity:

$$D_{1,z} = D_{2,z}, B_{1,z} = B_{2,z}, E_{1,x,y} = E_{2,x,y}, H_{1,x,y} = H_{2,x,y}$$

\rightarrow no transverse-electric mode (TE)

\rightarrow transverse-magnetic mode (TM)



"Ansatz" for fields along \hat{e}_x ($j=1,2$):

$$\vec{E}_j = (E_{j,x}, 0, E_{j,z}) e^{i(\vec{k}_j \cdot \vec{r} - \omega t)}$$

$$\vec{H}_j = (0, H_{j,y}, 0) e^{i(\vec{k}_j \cdot \vec{r} - \omega t)}$$

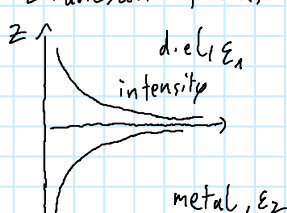
$$\vec{D}_j = \epsilon_0 E_j \vec{E}_j, \vec{B}_j = \mu_0 \vec{H}_j \quad \text{with } \vec{k}_j = (\beta_j, 0, k_{j,z}) \\ k_x = \text{const}$$

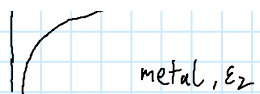
cont. + M-equ.

$$\frac{k_{1,z}}{\epsilon_1} = \frac{k_{2,z}}{\epsilon_2}$$

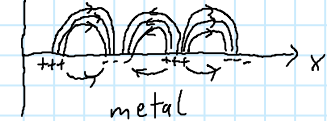
for solutions bound to interface: $k_{1,z} = +ix_1, k_{2,z} = -ix_2$

\Rightarrow Fields: $\vec{E}_j \propto e^{\pm i x_j z}$ "Evanescent fields", near the surface \Rightarrow "electrical near fields"
 conditions $\epsilon_1' = -\epsilon_2'$





- Em wave in diel. & oscillating e⁻ plasma in metal
- Penetration depth $\sim \frac{\lambda}{2}$ in the medium & in metal given by skin depth δ

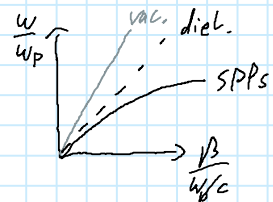


Dispersion relation of SPPs: $|\vec{k}_{1/2}|^2 = \epsilon_{1/2} k_0^2 = \beta^2 + k_{1/2z}^2 = \beta^2 - k_{1/2}^2$
 L vacuum $\frac{\omega}{c}$

$$\Rightarrow \beta = k_x = \frac{\omega}{c} \sqrt{\frac{\epsilon_1 \epsilon_2}{\epsilon_1 + \epsilon_2}}$$

Under assumption that in diel. $\epsilon_1(\omega) \approx \text{const.}$

metal with low damping $\epsilon_2(\omega) \approx 1 - \frac{w_p^2}{\omega^2}$



- SPPs cannot be excited by light, bc $\omega_{\text{light}} = \omega_{\text{SPP}}$ never when $\vec{k}_{\text{light}} = \vec{k}_{\text{SPP}}$

Components normal to the surface: $k_{j,z}^2 = \frac{\epsilon_j^2}{\epsilon_1 + \epsilon_2} k_0^2$

- Imaginary part of diel. causes Ohmic damping of e⁻ oscillations in metal

$$\Rightarrow \beta = \beta' + i\beta''$$

$$\Rightarrow \text{Solution of SPPs: } \vec{E}_2 = (E_{2,x}, 0, E_{2,z}) e^{i\vec{k}_2 \vec{r} - i\omega t} \text{ with damping term } \exp^{-\beta'' x}$$

$$\Rightarrow \delta_{\text{SPP}} = \frac{1}{2\text{Im}(\beta)}$$

$$\sqrt{a+ib} = \sqrt{\frac{ia^2+b^2+a}{2}} + i \text{sgn}(b) \sqrt{\frac{ia^2+b^2-a}{2}}$$

↓

Case of metal films of thickness d:



- Two interfaces to diel. substrate
- Thick metal film → two independent SPPs, depending on diel. const. of diel.
- Thin metal film → Coupling between SPPs → ω_{SPP} split into two branches (symmetric: low freq., antisym.: high freq.)

$$\omega_{\pm} = \omega_{\text{SPP}} \sqrt{1 \pm \exp(-\beta d)}$$

Configurations for the excitation of SPPs:

Direct excitation of SPPs by light only possible by following techniques:

- Prism coupling: Prism coated with thin film (Kretschmann config.)

Direct excitation of SPPs by light only possible by following techniques:

- Prism coupling: Prism coated with thin film (Kretschmann config.) or with small air gap (O^{Hg})
- Grating coupling: Phase matching by grating on surface with $\beta = k \sin \theta \pm n_g \frac{2\pi}{a}$ "grat. const"
- Strong focused light: large range of angles with different k' 's
- Near-field excitation: metal-tip \rightarrow SPPs can be launched
- Coupling to photonic elements: SPPs can be launched by coupling to wave guides/optical fibres

"1D" surface plasmons

By restricting the sample size, formed by dielectric/metal/dielectric or metal/dielectric/metal structures
(such as gaps, V-grooves, ridges)

- SPPs are non-radiative modes \Rightarrow no direct observation (SNOM)

3.4 Localized surface plasmons (particle plasmons)

Metal particles in order of/below λ

Collective oscillations of free e^- confined to geometric dim. of nanostructures

\Rightarrow Localized surface plasmon polaritons (LSPPs)

External field can penetrate into volume & shift the conduction e^-

\Rightarrow dipole-like charge separation

Coherently shifted e^- + restoring field = oscillator def. by m_e^* , charge density & geometry of particle

\Rightarrow Plasmon resonance

Plasmon resonances of small spherical particles

Assumption in LSPP model:

- Sphere of rad. a in static el. field $\vec{E}_{\text{in}} = E_0 \hat{e}_z$

- Surrounding medium is isotropic & non-absorbing with ϵ_d

- Metal described by compl. ϵ_s

- El. field $\vec{E} = -\nabla \phi$ by solving $\Delta \phi = 0$ in spherical coord.

$$\text{Laplace eqn. : } \frac{1}{r^2 \sin \theta} \left[\sin \theta \partial_r (r^2 \partial_r) + \partial_\theta (\sin \theta \partial_\theta) + \frac{1}{\sin \theta} \partial_\phi^2 \right] \phi(r, \theta, \phi) = 0$$

$$\text{Azimuthal symm. } \Rightarrow \phi_s(r, \theta) = \sum_{l=0}^{\infty} A_l r^l P_l(\cos \theta); \quad \phi_d(r, \theta) = \sum_{l=0}^{\infty} (B_l r^l + C_l r^{l-1}) P_l(\cos \theta)$$

$\begin{matrix} \text{Inside sphere} & \text{Legendre poly} & \text{Outside the sphere} \end{matrix}$

$$\phi_d = \phi_{\text{scatter}} + \phi_o$$

$$\text{Boundary cond. at } r=a: \partial_\theta \phi_i = \partial_\theta \phi_d \quad \& \quad \epsilon_s \partial_r \phi_s = \epsilon_d \partial_r \phi_d$$

Boundary cond. at $r=a$: $\partial_\theta \Phi_i = \partial_\theta \phi_k$ & $\epsilon_s \partial_r \phi_i = \epsilon_k \partial_r \phi_k$

$$\Rightarrow \phi_s(r, \theta) = -\frac{3\varepsilon_d}{\varepsilon_s + 2\varepsilon_d} E_0 r \cos \theta$$

$$\Phi_d(r, \theta) = -E_0 r \cos \theta + \frac{\vec{p} \cdot \hat{r}}{4\pi \epsilon_0 \epsilon_d r^3} \quad \text{with } \vec{p} = 4\pi \epsilon_0 \epsilon_d a^3 \frac{\epsilon_s - \epsilon_d}{\epsilon_s + 2\epsilon_d} E_0 \quad \text{"dipole moment"}$$

$$\Rightarrow \vec{E}_s = \frac{3\epsilon_0}{\epsilon_s + 2\epsilon_0} \vec{E}_0 \quad \& \quad \vec{E}_d = \vec{E}_0 + \frac{1}{4\pi\epsilon_0\epsilon_d} \frac{3\vec{n}(\vec{n} \cdot \vec{p}) - \vec{p}}{r^3} \quad \text{with } \vec{n} = \frac{\vec{r}}{r}$$

Polarizability def. by $\vec{p} = \epsilon_0 \epsilon_d \alpha \vec{E}_0$ becomes $\alpha = 4\pi \epsilon_0 a^3 \frac{\epsilon_s - \epsilon_d}{\epsilon_s + 2\epsilon_d}$

Scattering crosssection of sphere obtained by tot. radiated power/intensity of exciting wave

$$P = \frac{w^4}{12\pi\varepsilon_0\varepsilon_d C^3 |p|^2} \quad , \quad I = \frac{1}{2} C \varepsilon_0 \varepsilon_d E_0^2$$

$$\Rightarrow \sigma_{\text{scat}} = \frac{k^4}{6\pi^2 E_0} |\alpha(\omega)|^2 = \frac{8\pi}{3} k^4 \alpha^6 \left| \frac{\epsilon_s - \epsilon_d}{\epsilon_s + 2\epsilon_d} \right|^2$$

! Redshift of resonance with increasing diel. const of diel. environment

Power loss due to scattering & absorption of plasmons "extinction"

↳ corresponds to dissipated power by a point dipole $P_{\text{abs}} = \frac{\omega}{2} \text{Im}(\vec{\mu} \cdot \vec{E}_0^*)$ with $\vec{\mu} = \epsilon_0 \vec{E}_0$

$$\Rightarrow \sigma_{abs} = \frac{k}{\epsilon_0} \text{Im}(\alpha \epsilon_0) = 4\pi k a^3 \text{Im}\left(\frac{\epsilon_s - \epsilon_d}{\epsilon_s + 2\epsilon_d}\right)$$

Large particles: scattering dominates (a^6)

smaller : Extinction (a³)

\Rightarrow Transition \rightarrow color change

Influence plasmon resonance (\rightarrow "color") by:

- Choice of material (metal)
 - Choice of dielectric medium
 - Geometry of nanoparticle
 - Shape
 - Aspect ratio : Dichroism in elliptical particles (shorter & longer wavelength)

3.5 Applications of plasmonics

3.5.1 Optical antennas

Concentrating energy of external em wave at location of nanoparticle or tip

\Rightarrow Oscillation of free e^- density \Rightarrow charge carrier flux

\Rightarrow Oscillation of free e^- density \Rightarrow charge carrier flux
 Structure acts as point dipole & emits dipole radiation [characteristics of an antenna]
 [metallic nanostructures with plasmon resonance in UV/vis/near IR is called optical antenna]
 Some examples:

- Surface and tip Raman spectroscopy
- Fluorescence enhancement
- SPP & LSPP sensors in bio, med., chem.
- opto electronic devices (LEDs, solar cells)
- Information technology
- ⋮

3.5.2 Near-field scanning optical microscopy

Near-field (scanning optical) microscopy NSOM/SNOM

- Sharp tip into near vicinity of a surface
- Tip couples with evanescent near-field of sample
- Emitted photons detected
 - ... as propagating modes in fiber (NSOM)
 - ... scattered into far field by massive metal tip (no NSOM)

Optimization:

- light harvesting antenna
- smaller dimensions \rightarrow higher resolution
- mechanical / chem. stability

3.5.3 Resonance shift sensors

SPP sensors

Kretschmann configuration at resonance angle $\Theta_0 \rightarrow$ SPPs excited at gold interface
 If layer of molecules is absorbed onto surface \Rightarrow eff. refractive index of med. \nearrow
 $\Rightarrow \Theta_0$ shifts to larger Θ_n
 [Θ_0 can be restored]

LSPP sensors

- well def. plasmon resonances
- Absorption of molecules changes effective refractive index of medium
 \Rightarrow Shift of resonance to longer λ ($\Delta\lambda$)
- Maximum $\Delta\lambda_{\max} = M \Delta n_{\text{eff}} (1 - e^{-2d/b})$

\Rightarrow Shift of resonance to longer λ ($\Delta\lambda$)

• Maximum: $\Delta\lambda_{\max} = m \Delta n_{\text{eff}} (1 - e^{-2d/l_d})$
L sensitivity

3.5.4 Surface-enhanced Raman spectroscopy (SERS)

Principle: Locally enhanced near-field at single or between several optical antennas

\rightarrow Raman intensity \uparrow for single molecules

L must be placed in "hot spots" of high field strength

Enhancement factor: $EF_{\text{SERS}} = \frac{|E_{\text{in}}(\omega)|^2 / E_{\text{out}}(\omega - \omega_0)|^2}{E^4}$ ← near-field upon incidence & Stokes shifted (emitted)
L Incoming em.wave

nano particles in solution $\rightarrow = \frac{I_{\text{SERS}}(\omega_0) / N_{\text{surf}}}{I_{\text{NRS}}(\omega_0) / N_{\text{vol}}} \uparrow$
with Raman

At surface $\rightarrow = \frac{I_{\text{SERS}}(\omega_0) / A_{\text{SERS}}}{I_{\text{NRS}}(\omega_0) / A_0} \uparrow$ area of hot spots
L regular L focus area

3.5.5 Tip-enhanced Raman spectroscopy (TERS)

Exists

3.6 Photonic crystals

Are structures with periodically varying dielectric const ($\lambda \approx 1.5 \text{ nm}$, periodicity $\approx 500 \text{ nm}$)

\Rightarrow Photonic band gaps (forbidden frequency ranges which cannot scatter)

L analogous to electronic bandgaps

Can be calculated with M-equations 1D analogous to Bragg lattice

1D:

• Infinite layers of thickness d , $\hat{n} \parallel \hat{e}_z$, alternating ϵ_1, ϵ_2 , wavevector of light $\vec{k} = (k_x, k_y, k_z)$

• Def. TE/TM modes

- $\vec{E} \parallel \text{interface}$: $\vec{E}(z) = E(z) \exp(i(k_x x + k_y y)) \hat{n}_x$

- $\vec{H} \parallel \text{interface}$: $\vec{H}(z) = H(z) \exp(i(k_x x + k_y y)) \hat{n}_x$?

In each layer, solution for $E(z), H(z)$ are superpositions of forwards & backwards propagating wave

with $k_{\perp j} = \sqrt{\frac{\omega^2}{c^2} \epsilon_j - k_{||j}^2}$, $k_{||j} = \sqrt{k_x^2 + k_y^2}$

At $z_n = nd$:

TE: $E_{n,1}(z_n) = E_{n+1,2}(z_n)$, $\frac{dE_{n,1}(z)}{dz} = \frac{dE_{n+1,2}(z)}{dz}$

TM: $H_{n,1}(z_n) = H_{n+1,2}(z_n)$, $\frac{1}{\epsilon_1} \frac{dH_{n,1}(z)}{dz} = \frac{1}{\epsilon_2} \frac{dH_{n+1,2}(z)}{dz}$

$$TM: H_{n,m}(z_n) = H_{n+1,2}(z_n) \quad , \quad \frac{1}{\epsilon_1} \frac{dH_{n,1}(z_n)}{dz} = \frac{1}{\epsilon_2} \frac{dH_{n+1,2}(z_n)}{dz}$$

$$\Rightarrow \text{Characteristic equation: } \cos(2k_B d) = \cos(k_{z1} d) \cos(k_{z2} d) - \frac{1}{2} (p_m + \frac{1}{p_m}) \sin(k_{z1} d) \sin(k_{z2} d)$$

$$\text{with } p_m = \frac{k_{z2}}{k_{z1}} \text{ for TE modes; } p_m = \frac{k_{z2}}{k_{z1}} \frac{\epsilon_1}{\epsilon_2} \text{ for TM modes}$$

Defects:

- Light localized or directed with help of crystal defects
- Photons with energies within band gap can only propagate through defect lines

2D

Fully reflect light \rightarrow Perfect mirrors

1D Waveguide

QD Resonators with high Q (Quality factor) $Q = \frac{\omega_0}{\Delta\omega}$ ↑ resonance, used for light trapping

└ FWHM

3.7 Metamaterials

Lit.: p. 129

Artificial materials with spatial variations of $\epsilon(\vec{r}), \mu(\vec{r}) \Rightarrow$ distortions in $\vec{D}, \vec{B}, \vec{S}$

Invisibility cloaks

Coord. trafo $\vec{x} \rightarrow \vec{u} \Rightarrow$ M. eqs. unchanged but ϵ, μ vary as function of $(\frac{\partial x_i}{\partial u_j})$

Example:

Trafo for sphere with rad R_1 : $r < R_2 \rightarrow R_1 < r < R_2$

Trafo: $r' = R_1 + r(R_2 - R_1)/R_2$, $\theta' = \theta$, $\varphi' = \varphi$

In $R_1 < r < R_2$:

$$\epsilon_{r'}^i = \mu_{r'}^i = \frac{R_2}{R_2 - R_1} \frac{(r' - R_1)^2}{r'} ; \quad \epsilon_{\theta'}^i = \mu_{\theta'}^i = \epsilon_{\varphi'}^i = \mu_{\varphi'}^i = \frac{R_2}{R_2 - R_1}$$

$$r > R_2: \quad \epsilon_r^i = \mu_r^i = \epsilon_r^i = \mu_r^i (= \epsilon_{r'}) \stackrel{r > R_2}{=} \mu_{r'}^i = \dots = 1$$

Ex. 2 p. 131

Negative refractive index $n < 0$:

Refract light negatively

3.8 Single photon emitters

Lit.: p. 133

Lit.: p. 133

Production via 2 level system, antibunching

Emission of one photon rules out emission of second

Mode of el. field is quantized as h.o.

2nd. order correlation function: $g^{(2)}(\tau) = \frac{\langle I(t+\tau) I(t) \rangle}{\langle I(t) \rangle^2}$

Detection:

Hanbury-Brown-Twiss interferometer

split photon field \Rightarrow Wave function collapses

In case of ideal bunching: $g^{(2)}(0) = 0$, $g^{(2)}(\tau) > g^{(2)}(0)$

Ideal single-photon source

- Single photon on demand
- 100% single photon
- 0% more

Realizations of single photon sources (SPS)

Two level system

Deterministic (external excitation)

- Nano diamond
- SC QDs
- Single atoms
- Single molecules

Probabilistic

Random emission of entangled photon pairs from crystals, waveguides or fibers

$$0 = e(N_D^- + N_A^+ - n - p)$$

Zusammenfassung Chapter 4

Freitag, 22. Juli 2022 11:27

4. Electronic properties of nanostructures: Tunneling & Josephson effects

4.1 Tunneling effects (metals, supercond.)

4.1.1 Tunneling through barriers & metallic tunnel junctions

Tunneling effect based on probability density 4^*4 for cont. WF ψ

→ met./vac. interface at $x=0$: WF for $e^- \rightarrow E_F$ does not disappear outside the met.

$$\text{Amplitude decays wr } |4| \propto e^{-kx} \text{ wr "inverse decay length" } x \approx \left(\frac{2m}{\hbar^2}\right)^{1/2} \phi^{1/2}$$

└ Work function

In the following:

I: Insulator barriers

N: metallic - normal conductor

F: Ferromagn.

S: Superconducting

↓

• For tunneling of quasipart. between SC electrodes :: DOS modified

• emergence of energy gap in excitation spectrum has important role

• ↳ F-electrodes: Disappearance of degeneracy of spin states in DOS important

Basic distinctions:

- Elastic vs. inelastic

Elastic: Energy of e^- doesn't change during tunneling

Inelastic: e^- gains/loses energy due to excitation/absorption (phonons, magnons, plasmons, ...)

- 1D vs. 3D

↳ often for simplification

1D: Good approx for planar junction

3D: other structures (e.g. tip on planar surface)

- rectangular pot. barrier vs. arbitrarily shaped pot. barrier

↳ much more easily (but bad approx. for real tunneling)

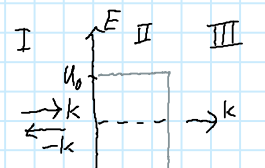
Applications

- Tunneling spectroscopy

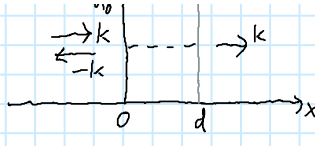
- Devices (Josephson junction, magn. tunnel junc. ...)

Elastic tunneling through 1D rectangular barrier

$$I: -\frac{\hbar^2}{2m} \frac{\partial^2 \psi_I}{\partial x^2} = E \psi_I \quad \text{wr } \psi_I = e^{ikx} + A e^{-ikx} \quad \text{wr } k^2 = \frac{2mE}{\hbar^2}$$



$$I: -\frac{\hbar^2}{2m} \frac{\partial^2 \psi_I}{\partial x^2} = E \psi_I \quad \text{w.r.t. } \psi_I = e^{ikx} + A e^{-ikx} \quad \text{w.r.t. } k = \frac{\sqrt{2mE}}{\hbar}$$



$$II: -\frac{\hbar^2}{2m} \frac{\partial^2 \psi_{II}}{\partial x^2} + U_0 \psi_{II} = E \psi_{II}$$

$$\Rightarrow \psi_{II} = B e^{-kx} + C e^{kx} \quad \text{w.r.t. } k^2 = \frac{2m(U_0 - E)}{\hbar^2}$$

$$III: -\frac{\hbar^2}{2m} \frac{\partial^2 \psi_{III}}{\partial x^2} = E \psi_{III} \quad \text{w.r.t. } \psi_{III} = D e^{ikx}$$

Ratio of trans (ψ_{II}) to incident (ψ_I) e^- current \Rightarrow transmission coeff. & tunneling prob.

$$T_m = \frac{|D|}{|A|} = |D|^2 \quad \text{"Probability of } e^- \text{ tunneling through barrier"}$$

w.r.t. boundary cond. (continuity of ψ & $\frac{\partial \psi}{\partial x}$ at interfaces $x=0, d$)

$$d \gg x^{-1} \quad \Rightarrow T_m = \left(\frac{4kx}{k^2 + k^2} \right)^2 e^{-2kd} \quad \rightarrow \text{probability } \downarrow \text{ w.r.t. thickness } d \uparrow \quad \text{Exponentially, even for small variations.}$$

$$\text{Inverse decay length } x = \frac{\sqrt{2m(U_0 - E)}}{\hbar} \quad \text{from eff. height of pot. barr. } (U_0 - E)$$

$$\rightarrow \text{Typically: } (U_0 - E) \approx \text{eV} \Rightarrow \frac{1}{x} \approx 1 \text{ Å}$$

Tunneling current I as function of applied voltage V

Measured quantities in experiments:

- Tunneling current $I(V)$

$$\rightarrow \text{Diff. tunneling conductance } G(V) = \frac{\partial I}{\partial V}$$

- \rightarrow Inverse $\frac{\partial V}{\partial I}$ (tunneling resistance) as function of V

$V=0$: E_F equ. on both electrodes

$V \neq 0$ (applied) \rightarrow energy difference eV between two E_F 's

Convention:

Pos. volt. V lowers right electrode w.r.t. respect to left

For elastic tunneling processes:

$$\text{Fermi dist. } F(\epsilon) = \frac{1}{\exp(\epsilon/k_B T) + 1}$$

$$\text{Tunneling current } I_{12} \propto \int_{-\infty}^{\infty} T_m(\epsilon) D_1(\epsilon - eV) f(\epsilon - eV) D_2(\epsilon) \{1 - f(\epsilon)\} d\epsilon \quad \text{from left to right}$$

$$I_{21} \propto \int_{-\infty}^{\infty} T_m(\epsilon) D_2(\epsilon) f(\epsilon) D_1(\epsilon - eV) \{1 - f(\epsilon - eV)\} d\epsilon \quad \text{right to left}$$

$$\Rightarrow \text{Net tunneling current: } I \equiv I_{12} - I_{21} \propto \int_{-\infty}^{\infty} T_m(\epsilon) D_1(\epsilon - eV) D_2(\epsilon) [f(\epsilon - eV) - f(\epsilon)] d\epsilon$$

NIN-junction

Assumptions:

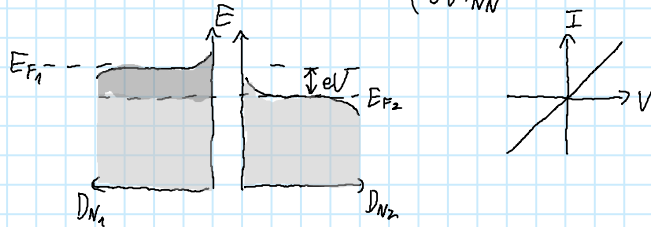
- $D_{N_{12}}(E) = D_{N_{12}}(E_F) = \text{const.}$ \rightarrow e.g. free e^- gas in 3D

- $T_{N_{12}} = T_{N_{12}} = \dots$

- $D_{N_{1,2}}(E) = D_{N_{1,2}}(E_F) = \text{const.}$ e.g. free e^- gas in 3D
- $T_m(E) = T_m(E_F) = \text{const}$ high barrier independent on V_s

$$\Rightarrow I \propto \underbrace{D_{N_1}(E_F) D_{N_2}(E_F) T_m(E_F)}_{\text{const}} \int_{-\infty}^{\infty} [f(E-eV) - f(E)] dE$$

\Rightarrow Linear tunneling characteristics $\left(\frac{\partial I}{\partial V}\right)_{V=0} \equiv G_{NN} \propto D_{N_1}(E_F) D_{N_2}(E_F) \approx \text{const.}$



Appendix: Tunneling w/ finite barrier height p. 8

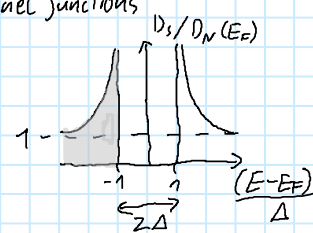
4.1, 2 Superconductors: Quasiparticle tunneling

Elastic tunneling of unpaired e^- in NIS & SIS tunnel junctions

Baldeen - Cooper - Schrieffer (BCS) theory:

$$D_s(\epsilon) = D_N(0) \frac{|E|}{\sqrt{\epsilon^2 - \Delta^2}} \quad |\epsilon| \geq \Delta$$

$$D_s(\epsilon) = 0 \quad |\epsilon| < \Delta$$

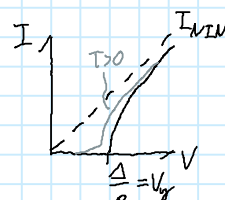
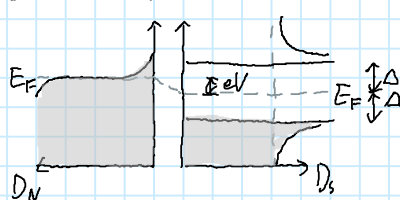


w/ Δ : Energy gap for quasipart. excitations in Sup. Cond. (from now SC)

D_N : DOS of mat. in normal conducting state

$$\epsilon = E - E_F$$

NIS-junction



$|V| < \frac{\Delta}{e}$: No tunneling current ($T=0$) or small ($T>0$)

$eV = \Delta$: tunneling current increases strongly, occu. states at E_F in N are facing high dens. of unocc. in S

$eV \gg \Delta$: $I_{NIS} \rightarrow I_{NIN}$

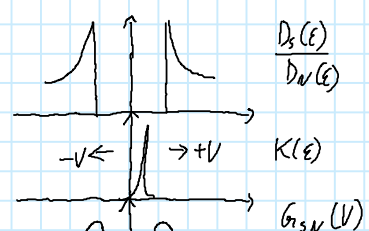
Assumption:

$$D_N(\epsilon) = D_N(0) = \text{const.} \quad \text{w/ } \epsilon = E - E_F$$

\Rightarrow Tunneling current $I \propto D_N(0) \int_{-\infty}^{\infty} D_s(\epsilon) [f(\epsilon - eV) - f(\epsilon)] d\epsilon$

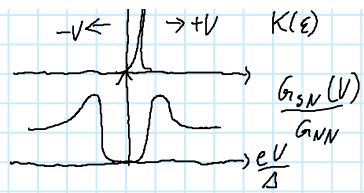
Diff. cond.

$$G_{SN}(V) \propto \int_{-\infty}^{\infty} D_s(\epsilon) K(\epsilon - eV) d\epsilon$$



Diff. cond.

$$G_{SN}(V) \propto \int_{-\infty}^{\infty} D_s(\epsilon) K(\epsilon - eV) d\epsilon$$



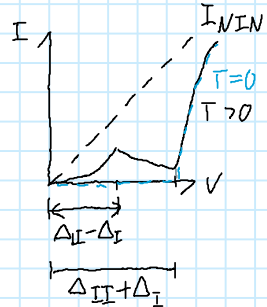
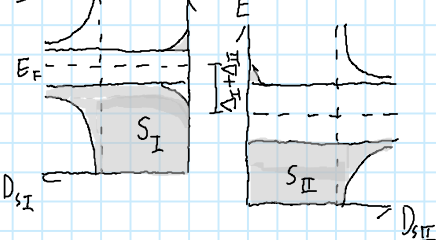
$K(\epsilon - eV)$: Derivative of Fermi dist. $f(\epsilon - eV)$

$$K = e\beta \frac{\exp[\beta(\epsilon - eV)]}{\{1 + \exp[\beta(\epsilon - eV)]\}^2} \quad \text{w/ } \beta \equiv \frac{1}{k_B T}$$

SIS-junction

With diff. energy gaps: $\Delta_I < \Delta_{II}$

for $eV = \Delta_{II} - \Delta_I$



$eV = \Delta_{II} - \Delta_I$: Therm. excited states in S_I facing high dens. of unocc. states in S_{II}

Disappear for $T \rightarrow 0$

$eV = \Delta_{II} + \Delta_I$: High dens. in S_I facing high dens. of S_{II}

If mat. of S_I & S_{II} are equal $\Rightarrow V_g = \frac{2\Delta}{e}$

4.2 Josephson effects & SQUIDs

4.2.1 Weak superconductivity: Josephson effects

Now: Cooper pairs

Described by macrosc. WF $\Psi = \Psi_0 e^{i\phi}$ w/ ampli Ψ_0 , phase ϕ

$$|\Psi_0|^2 \propto n_s$$

Cooper pair density

Supercurrent dens.: $\vec{j}_s = \frac{q_s n_s}{m_s} (\hbar \vec{\nabla} \phi - q_s \vec{A})$ w/ $\vec{B} = \nabla \times \vec{A}$, $q_s = 2e$, $m_s = 2m_e$

Def.: Gauge-invariant phase gradient:

$$\vec{\nabla} \phi = \vec{\nabla} \phi - \frac{q_s}{\hbar} \vec{A} \Rightarrow \vec{j}_s = \frac{q_s n_s}{m_s} \hbar \vec{\nabla} \phi$$

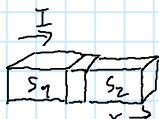
Gauge-invariant phase: $\phi(\vec{r}) = \varphi(\vec{r}) - \frac{q_s}{\hbar} \int_{\vec{r}_0}^{\vec{r}} \vec{A} d\vec{r}$

Consider S_1, S_2 w/ $\Psi_1 = \Psi_{0,1} e^{i\phi_1}$, $\Psi_2 = \Psi_{0,2} e^{i\phi_2}$

S1/barrier/S2 confi.:

barrier plane L_x , cross sect. $A_j = \text{const.}$

in ... linear range T

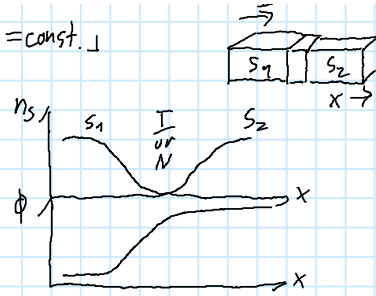


Γ barrier plane $L \times$, cross sect. $A_3 = \text{const.}$

Injecting const. I

$$\Rightarrow j_s(x) = \frac{I}{A_3} = \text{const.}$$

$$\Rightarrow n_s(x) \cdot \frac{\partial \phi}{\partial x}(x) = \text{const.}$$



n_s small (D, p)

$\Rightarrow \frac{\partial \phi}{\partial x}$ large $\Rightarrow \phi(x)$ makes step

thin barrier $\rightarrow n_s \rightarrow 0 \Rightarrow \phi(x)$ makes jump

\Rightarrow Weak Link char. by:

$$\text{Phase difference } \delta = \phi_2 - \phi_1 = \varphi_2 - \varphi_1 - \frac{q_s}{\hbar} \int_1^2 A_x dx$$

$$\Rightarrow j_s = j_s(\delta)$$

• ϕ_i is mod. 2π

$\Rightarrow j_s$ per. in δ

$$j_s = \sum_n j_{\text{on}} \sin n\delta + \sum_n j_{\text{off}} \cos n\delta \quad (n \in \mathbb{N})$$

• Time reversal invariance

$$\left. \begin{array}{l} j_s \rightarrow -j_s \text{ upon time reversal} \\ \delta \rightarrow -\delta \end{array} \right\}$$

$$j_s(\delta) = -j_s(-\delta) \quad \text{and} \quad j_s = \sum_n j_{\text{on}} \sin n\delta$$

• Often fast convergence $j_{\text{on}} \ll j_{\text{on}}$ for $n > 1$

$$\Rightarrow j_s = j_0 \sin \delta \quad 1. \text{ Josephson equ.}$$

Γ Supercurrent across barrier = "Josephson current"

In SIS: tunneling of Cooper pairs

$\delta = \delta(t) \Rightarrow \frac{\partial \delta}{\partial t} = \dot{\delta} \rightarrow$ volt. drop U across barrier & $\Phi \equiv \frac{\hbar}{2e}$ magn. flux quant.

$$\boxed{U = \frac{\hbar}{2e} \dot{\delta} = \frac{\Phi_0}{2\pi} \dot{\delta}} \quad 2. \text{ Josephson equation}$$

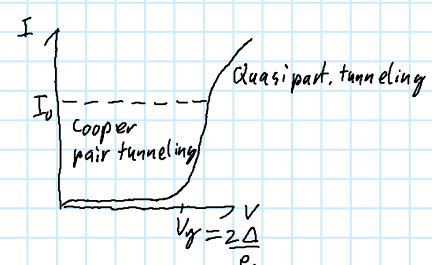
Consequences from Josephson eq.

$$U=0: \Rightarrow \delta = \text{const.} = \delta_0 \Rightarrow j_s = j_0 \sin \delta_0$$

max. value: $\sin \delta_0 = 1 \Rightarrow j_{s,\text{max}} = j_0$

\rightarrow Supercurrent, crit. curr. dens. $j_0 \ll j_c$, pair breakup

\rightarrow "Weak supercond."



$$U=\text{const.} \Rightarrow \boxed{\delta(t) = \delta_0 + \frac{2\pi U}{\Phi_0} t}$$

St linear \rightarrow T

$$\Rightarrow \boxed{j_s = j_0 \sin(\delta_0 + w_J t)}$$

$$\text{with } \boxed{w_J = \frac{2\pi}{\Phi_0} U}$$

\Rightarrow Coop-pair alternating current \rightarrow Josephson freq. $f_J = \frac{w_J}{2\pi} = \frac{U}{\Phi_0} = \frac{2eU}{h}$

\rightarrow Volt. controllable high freq. source

\rightarrow Const. $\boxed{\Phi_0 = h}$ \rightarrow fundamental physical const.

→ Volt. controllable high freqn. source

→ Const. $\phi_0 \equiv \frac{h}{2e}$ → fundamental physical const.

→ Effect used to def. [V]

$$[QHE]: R_H = \frac{1}{n} \frac{h}{e^2}$$

Interpretation: Phases of WFs ψ_i run against each other

Jos. altern. curr. \Leftrightarrow interference of waves in time

[Some Jos. types p. 17]

[Often used: Nb/Al-AlO_x/Nb ($T < 4K$)]

Current voltage char. of Jos. junct.

Description by: RCSJ model = resistively & capacitively shunted junction model



• Jos. current $I_s = I_0 \sin \delta$

• Displacement curr. through capacitance C if U flows t-dependent

$$I_d = C \dot{U}$$

• dissipative current contribution from quasipart.: $I_{qp} = \frac{U}{R}$

• Noise Current $I_N(t)$ through thermal noise in the resistance

$$\text{Kirchhoff: } I + I_N(t) = I_0 \sin \delta + \frac{U}{R} + C \dot{U} \quad [2nd eqn., U = \int \frac{\phi_0}{2\pi} \delta]$$

$$I + I_N(t) \approx I_0 \sin \delta + \frac{\phi_0}{2\pi R} \dot{\delta} + \frac{\phi_0 C}{2\pi} \ddot{\delta}$$

$U \neq 0$, altern. Jos. currents:

→ $I_{qp}(t)$ oscillates

→ high-freqn. volt. $U(t)$ wr dc volt. contribution

$$V = \langle U \rangle = \frac{1}{T} \int_0^T U(t) dt$$

Sol. of DGL $\Rightarrow S(t) \Rightarrow U(t) \Rightarrow V \Rightarrow$ (dc) curr.-volt.-char. $I(V)$

Analogous sys.: point-like part. in tilted washboard pot.

Phase diff. S can be descr. as part. in 1d-pot. along the coord. δ

$$\left[\frac{\phi_0}{2\pi} C \ddot{\delta} + \frac{\phi_0}{2\pi} \frac{1}{R} \dot{\delta} = -I_0 \sin \delta + (I + I_N) \equiv -\frac{2\pi}{\phi_0} \frac{\partial U_3}{\partial \delta} \right]$$

w tilted washboard pot. $U_3 \equiv \frac{\phi_0}{2\pi} \{ I_0 (1 - \cos \delta) - (I + I_N) \delta \}$

w amplitude "Jos. coupling energy" $E_3 = \frac{I_0 \phi_0}{2\pi}$

$$\text{Eqn. above normalized: } u_3 \equiv \frac{U_3}{E_3} = 1 - \cos \delta - (i + i_N) \delta \quad \text{w } i = \frac{I}{I_0}, i_N = \frac{I_N}{I_0}$$

3

$$\text{Equivalent to eqn. of motion: } m\ddot{x} + \zeta \dot{x} = -\frac{\partial W(x)}{\partial x} + F_d + F_N = -\frac{\partial [W(x) - (F_d + F_N)x]}{\partial x}$$

Point-like part wr mass m & friction coeff ζ along axis x in Pot. $W(x)$

External driving force F_d

Thermal noise force F_N

$$F = F_d + F_N \Rightarrow U_m(F, x) \equiv W(x) - Fx \quad \text{tilted due to forces}$$

In short:

$$m\ddot{x} + \zeta \dot{x} = -\nabla W(x) + F_d + F_N \Leftrightarrow \frac{\Phi_0 C}{2\pi} \ddot{\delta} + \frac{\Phi_0}{2\pi R} \dot{\delta} = -I_o \sin \delta + I(t) + I_N(t)$$

velo. $\dot{x} \Leftrightarrow \dot{\delta} \left(\frac{\Phi_0}{2\pi} \right) = U$ voltage

force $F_d, F_N \Leftrightarrow I, I_N$ current

friction $\zeta \Leftrightarrow I/R$ conductance

mass $m \Leftrightarrow C$ capacitance

Static, $V=0$:

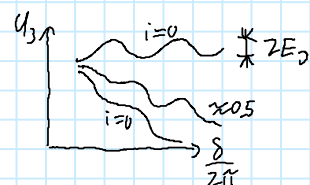
$I=0 \Rightarrow$ "Particle" is trapped in one minima of untilted cos-pot., oscil. wr plasma freq. $w_p = \left(\frac{2\pi}{\Phi_0} \frac{I_o}{C} \right)^{1/2}$

$$\langle V \rangle (\text{velo.}) = 0$$

dyn., $V \neq 0$

With $I \uparrow \Rightarrow$ height of barrier to next loc. min \downarrow

Until $I=I_o \Rightarrow$ Loc. mins disappear & 'part.' moves with finite velo



Vgl. wr correction:

Effect of damping:

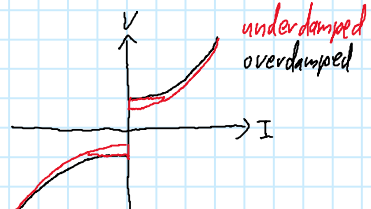
Strong damping: term $\zeta \dot{\delta}$ dom., decreasing $I \rightarrow I_o \Rightarrow$ minima appear again \Rightarrow part. immediately trapped
 \rightarrow Non hysteretic IV-Char.

Weak damping: Mass plays key role, even if $I < I_o$ (local max/min have formed) part can move
 \rightarrow Junction remains at $V \neq 0$ until "retrapping state" $I_r < I_o$

\rightarrow hysteretic IVC wr Stewart-McCumber-Para β_c

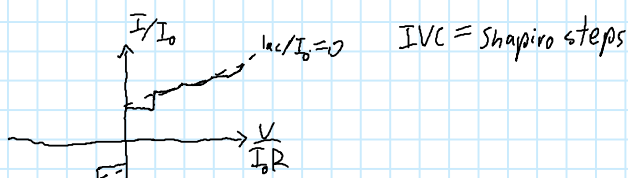
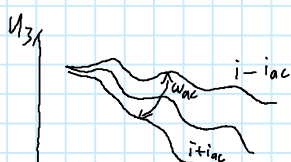
$$(f = \tau w_c \text{ wr } w_c = \frac{2\pi}{\Phi_0} I_o R)$$

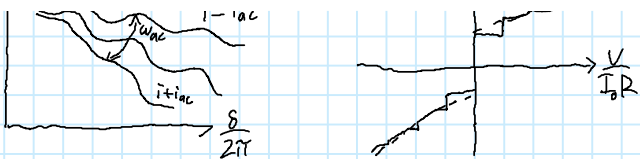
$$\beta_c \ddot{\delta} + \dot{\delta} + \sin \delta = i + i_N \text{ wr } \beta_c = \left(\frac{w_c}{w_p} \right)^2 = \frac{2\pi}{\Phi_0} I_o R^2 C$$



Dynamics under the influence of an alternating current

Case of driving curr. $I_{tot} = I + I_{ac} \sin \omega_{ac} t$ wr dc-comp. I, ac wr ampli. I_{ac} & freq. $f_{ac} = \omega_{ac}/2\pi$





Appropriate cond.: Motion of "part" sync. w ext. excitation

$$\Rightarrow \text{Change of } \delta \text{ by } n_2 \tilde{\nu} \text{ per excit. per. } T_{ac} = \frac{2 \tilde{\nu}}{\omega_{ac}}$$

$$\Rightarrow V_{dc} \text{lo } i = \frac{n Z_1 Y}{T_{ac}} = n w_{ac}$$

• Stable in certain regions of tilt angle

↳ average velo (dc) only given by frequ. of ac drive

↳ independent on value of average tilt angle (i_{dc})

\Rightarrow Current steps of const. volt.

$$V_n = \frac{\phi_0}{2\pi} \dot{s} = n \frac{\phi_0}{2\pi} w_c = n V_1 \quad \text{where} \quad V_1 \equiv \phi_0 / 4\pi$$

Josephson junction in magn. field

function in ext. field \vec{F} , plane of barrier: (x, y) ; $I \parallel \hat{e}_z$

magn.-field penetrate barrier homogeneously for small junction length $\approx \lambda_L$

Thickness of super-cond. electrodes $\gtrsim 2\lambda_L$

↳ London penetration depth

\rightarrow magn. flux $\propto B = M_0 H$

$$\phi_3 = B (2\lambda_L + d) a = B d_{\text{eff}} a$$

length of junction
= $2\lambda_L + d$
barrier thickness

Rel. S & B:

$$\frac{\partial \delta}{\partial x} = 2\pi \frac{B_{0\text{eff}}}{\Phi_0} \Rightarrow \text{Phase } \uparrow \text{ linearly along junction grows linearly}$$

$$\Rightarrow S(x) = S(0) + \frac{2\pi}{\Phi_0} B_{\text{eff}} x$$

$$\Rightarrow j_s(x) = j_0 \sin \left[\delta(0) + \frac{2\pi}{\phi_0} B_{\text{eff}} x \right] \quad \text{in current per unit area } A_s = ab, \quad j_0 = \frac{I_0}{A_s}$$

\Rightarrow 3 os-curr. dens. osci. along junction

Wavelength depends on magn. flux $\phi_3 = B_{\text{eff}} u$

$$\text{If } \alpha \approx 4\lambda_3 \Rightarrow \text{Jos. penetr. depth } \lambda_3 = \sqrt{\frac{\Phi_0}{2\pi\mu_{\text{des}}}}$$

Total supercurrent through the junction

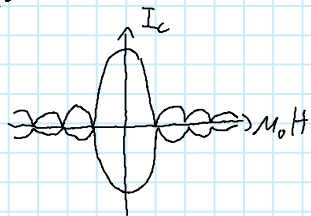
$$I_s = \int_0^b dy \int_0^a dx j_0 \sin S(x) = -j_0 b \left. \cos \left(S_0 + \frac{z\pi}{\phi_0} B_{\text{eff}} x \right) \right|_0^a$$

$$\text{Maximum super curr. } I_c \rightarrow \sin\left(\delta_0 + \frac{\pi}{2} \frac{\Phi_3}{\Phi_1}\right) \pm 1$$



$$\text{Maximum super curr. } I_c \rightarrow \sin(\delta_0 + \pi \frac{\Phi_3}{\Phi_0}) \pm 1$$

$$I_c(\Phi_3) = I_0 \left| \frac{\sin(\pi \frac{\Phi_3}{\Phi_0})}{\pi \frac{\Phi_3}{\Phi_0}} \right|$$



\Rightarrow Fraunhofer pattern

4.2.2 SQUIDs: Superconducting quantum interference devices

Basic principle

Supercond. loop w/ inductance L , which is intersected by one (rf) or two (dc SQUID) Joss. junc.

- Combine two effects: fluxoid quantization & Joss-effect

Result:

Periodic response to external flux Φ_a in:

- the max Joss. curr. I_c
 - $\langle V \rangle$ across Joss. junc. (dc SQUID)
 - ampli. V_{rf} of rf volt. of resonant circuit (rf SQUID)
- with period Φ_0 .

Sensitivity:

- flux noise $S_\phi^{1/2} \approx 1-10 \mu\Phi_0 / \sqrt{\text{Hz}}$
- magn. field noise: $S_B^{1/2} \approx 1-10 \text{ fT} / \sqrt{\text{Hz}}$
- energy res.: $\epsilon = S_\phi / 2L$

Basics of dc SQUID

a) Tot. flux in dc SQUID & circulating current

$$2\pi n = \oint \vec{B} \cdot d\vec{l}, \quad n \in \mathbb{Z} \quad (\text{from fluxoid quantizations})$$

Across two Joss. junc.

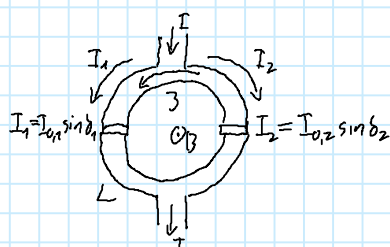
$$\Rightarrow \delta_2 - \delta_1 + 2\pi n = \underbrace{\frac{2\pi}{\Phi_0} (\Phi_a + L\beta)}_{= \Phi_T} \quad \text{w/ } \beta: \text{induced circulating curr.}$$

Def. of β :

SQUID biased at curr. $I \rightarrow$ splits into current I_1 & I_2 through the two arms: $I = I_1 + I_2$

$$\Rightarrow I_1 = \frac{I}{2} + \beta \quad \& \quad I_2 = \frac{I}{2} - \beta$$

$$\Rightarrow \text{Current circulating in the loop } \beta = \frac{I_1 - I_2}{2} \quad I_1 = I_{0,1} \sin \delta_1, \quad I_2 = I_{0,2} \sin \delta_2$$



b, d, SQUID - static case:

$$V=0 :$$

$$\text{1st equ. : } I_1 = I_0 \sin \delta_1, \quad I_2 = I_0 \sin \delta_2$$

$$\Rightarrow I = I_0 (\sin \delta_1 + \sin \delta_2) = 2 I_0 \cos \left(\frac{\delta_2 - \delta_1}{2} \right) \sin \left(\frac{\delta_1 + \delta_2}{2} \right)$$

$$\stackrel{\phi_T}{\Rightarrow} I = 2 I_0 \cos \left(\frac{\pi \phi_T}{\phi_0} \right) \sin \left(\delta_1 + \frac{\pi \phi_T}{\phi_0} \right)$$

Two analytical cases:

Screening parameter $\beta_L = \frac{2 I_0 L}{\phi_0}$ "Strength" of max. possible flux $\phi_{J,\max} = I_{\max} L = I_0 L$

(i) small inductance $\beta_L \ll 1$:

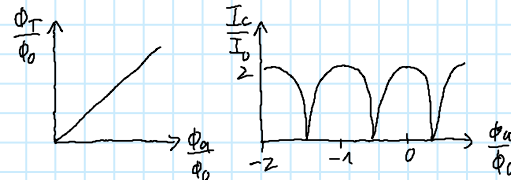
$$\Rightarrow \phi_T \approx \phi_a$$

$$\Rightarrow I \approx 2 I_0 \cos \left(\frac{\pi \phi_a}{\phi_0} \right) \sin \left(\delta_1 + \frac{\pi \phi_a}{\phi_0} \right) \text{ max for } \sin() = \pm 1$$

$$\Rightarrow I_c \approx 2 I_0 \left| \cos \left(\frac{\pi \phi_a}{\phi_0} \right) \right|$$

$$\rightarrow \text{In limit } \beta_L \ll 1 \Rightarrow \Delta I_c = 2 I_0$$

(ii) Appendix p.29



c) dc-SQUID - dynamic case

$V \neq 0$, const. bias curr. $I_B \gtrsim 2 I_0$, $V(\phi_a)$

$R_{1,2}, C_{1,2}$ play a role \Rightarrow RCSJ

$$\Rightarrow I_{c,\max} = 2 I_0 \text{ at } \phi_a = n \phi_0, I_{c,\min} \text{ at } \phi_a = \left(n + \frac{1}{2} \right) \phi_0$$

At bias curr. $I_B = \text{const.} \Rightarrow V$ oscillates

\Rightarrow SQUID works as flux to voltage converter

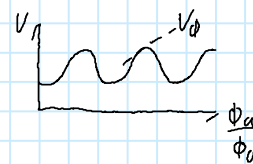
$$V_\phi \equiv \left(\frac{\partial V}{\partial \phi_a} \right)_{\max}$$

Small change $\delta \phi \Rightarrow \delta V = V_\phi \cdot \delta \phi$

Optimal case: $\beta_L \approx 1$

$$V_\phi \approx \frac{\Delta V}{\frac{1}{2} \phi_0} \approx \frac{R}{L}$$

• Flux noise: $S_\phi = \frac{S_V}{V_\phi^2}, \beta_L \approx 1 \Rightarrow S_\phi \approx 8 \phi_0 k_B T \frac{L}{I_0 R}$

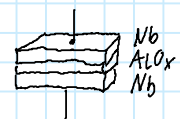


C. Practical SQUIDs

a) Fabrication

- Thin film

- Cooling via He at 4.2K for Nb/Al-AlO_x/Nb junctions



b) SQUIDs for measurements of magn. field & field gradients



Often interest in measuring $\delta B \Rightarrow \delta \phi_a = \delta B \cdot A_{\text{eff}}$

$\hookrightarrow \Delta \uparrow \rightarrow \text{non-linear c.n.l.}$

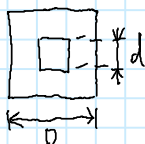
Often interest in measuring $\delta B \Rightarrow \delta \phi_a = \delta B \cdot A_{\text{eff}}$

For $A_{\text{eff}} \uparrow \Rightarrow$ Detectable $\delta B \downarrow$

$$S_B^{1/2} = S_\phi^{1/2} / A_{\text{eff}}$$

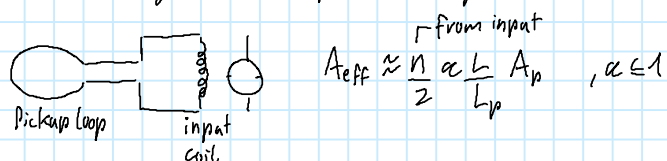
at same time small L

\Rightarrow Washer for focussing Flux



$$L = 1.25 \mu\text{m}, d, A_{\text{eff}} = d \cdot D$$

- Sensitive detection of magn. fields: superconducting flux transformer



$$A_{\text{eff}} \approx \frac{n}{2} \alpha \frac{L}{L_p} A_p, \alpha \leq 1$$

- Both: Input loop ontop of washer \Rightarrow Ketchen magnetometer \Rightarrow Sensitivity: $S_B^{1/2} \approx 1 \text{ FT} / \sqrt{\text{Hz}}$

$$\Rightarrow 1 \text{ FT} \cdot 60 \cdot 10^6 = \text{Earth magn. field}$$

Zusammenfassung Chapter05

Montag, 25. Juli 2022 14:11

05 Magnetic properties of nanostructure

5.1 Recap of Magnetism in the bulk

T dependence of Magnetization, Spinwave theory \rightarrow Bloch $T^{3/2}$ law

Dependence on dimension \rightarrow Shape, size important changes

5.2 What is Different in Nanomagnetism?

5.2.1 Why is nm-scale important in Magnetism

(i) $\leq 100 \text{ nm} \Rightarrow$ properties different than in the bulk

(ii) properties depend on sample size

- Size of MNPs characteristic lengths
- Broken translation symmetry at surf. & interface

\rightarrow modified DOS

\Rightarrow dependence on environment

\rightarrow Effects become more pronounced w.r.t. size!

- Modified excitation spec. of spin waves

Therm spin waves ($k_B T \approx E_{sw}$) $\rightarrow E_{sw} = \hbar \omega_{sw} = D_{sw} |k_{sw}|^2 \Rightarrow k_{sw} = \sqrt{\frac{k_B T}{D_{sw}}}$

- Modified dyn. prop.

Hysteresis loop for multi & monolayer

- thermal fluctuations

} MNPs \rightarrow superparamagnetism

5.2.2 Broken Translation symmetry

A: Dimensionality & DOS

Magnon - & electron DOS

- (i) Magnon

$$D(E) \propto \omega^{(d-n)/n} \quad \text{w.r.t. } n=2 \quad (\text{Dispersion of spinwaves in ferromagnetics})$$

- (ii) Electrons

Already done

$$\text{Conduction e- in scale of } \lambda_F = 2\pi \left(3\pi^2 n \right)^{-1/3}$$

$$\text{Pauli spin susceptibility: } \chi_p = \mu_0 \mu_B^2 D(E_F)$$

B: Reduced coordination number at surf & interfaces

Atoms at vac. interface have diff. number of nearest neighbours (NN)

5.2.3 Dimensionality & Phase transitions

- (i) Absolute value of Curie Temp. T_c :

(i) Absolute value of Curie Temp. T_c :

Magnetization reduction due to magnons diverges and at finite T they destroy ferromagn. order

$$M(T) = M(0) - \Delta M(T)$$

\hookrightarrow reduction due to therm. excited spinwaves

$$\Rightarrow \Delta M(T) \propto \int_0^{\infty} D(E) \cdot \frac{1}{e^{E/k_B T} - 1} dE \Rightarrow \text{Diverges for } T \text{ finite} \Rightarrow \text{breakdown of magn. order } (M(T)=0 \text{ for } T>0)$$

\hookrightarrow BC. Spinwaves are too easy to excite

Comments:

(i) isotropic interactions

If anisotropic \rightarrow easy axis \Rightarrow Disp. rel. in the form of $E = A + D_{\text{sw}} k^2$

$$\Rightarrow \Delta M(T) \propto \int_A^{\infty} \text{const.} \cdot \frac{1}{e^{E/k_B T} - 1} dE \text{ converges} \Rightarrow \text{magn. order stabilised}$$

(ii) short-range interactions

If long range, $E \propto \sqrt{k} k$ for small $k \Rightarrow D(E) \propto E^3$

$$\Rightarrow \Delta M \propto \int_A^{\infty} E^3 \frac{1}{e^{E/k_B T} - 1} dE \text{ doesn't diverge at } A \Rightarrow \text{magn. order may be stabilized}$$

(iii) $d=2$ or $d<2$

$$\Rightarrow D(E) \propto E^{5/2} \Rightarrow \Delta M(T) \text{ doesn't diverge}$$

(ii) Nature of transition

Ferromagn. near T_c :

$$\text{Specific heat } C \propto |T - T_c|^{-\alpha} \quad \alpha \approx 0$$

$$\text{saturation magnetization } M_s \propto |T_c - T|^{\beta} \quad \beta \approx .3$$

$$\text{magn. susceptibility } \chi \propto |T - T_c|^{-\gamma} \quad \gamma \approx 1 - \beta$$

5.3 Micromagn. Model & Magn. Domain

Size of part. can get to small to form magn. domain

5.3.1 Micromagn. model

Mat. always reaches locally saturation magnetization M_s , $|\vec{M}| = M_s$, orient. of $|\vec{M}|$ may vary

$$\text{Therm. equ. : } E_{\text{tot}}(\vec{H}_{\text{ext}}, \vec{M}) = U(\vec{M}) - \int M_0 \vec{H}_{\text{ext}} \cdot \vec{M} dV$$

\hookrightarrow internal energy

$$E_{\text{tot}} = E_z + E_{\text{ex}} + E_{\text{ms}} + E_A$$

Zeeman exchange magnstat. anisotropy

A. Zeeman:

$$E_z = -M_0 \int \vec{H}_{\text{ext}} \cdot \vec{M} dV \quad \text{"orient. of magn. Mom. along } \vec{H}_{\text{ext}}$$

$$\rightarrow \text{Energy dens. } e_z = -M_0 \vec{H}_{\text{ext}} \cdot \vec{M} \Rightarrow S dV$$

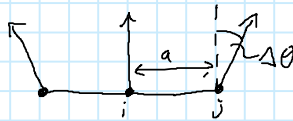
$\vec{B} = \mu_0 \vec{H}_{\text{ext}} + M$ or V orientation of magn. mom. along \vec{H}_{ext}

$$\rightarrow \text{Energy dens. } e_{\text{ext}} = -\mu_0 \vec{H}_{\text{ext}} \cdot M \propto \int dV$$

B. Exchange:

Exchange between two spins \vec{s}_i, \vec{s}_j : $E_{\text{ex},ij} = -2J \vec{s}_i \cdot \vec{s}_j$ w/ exch. const $J > 0$

W/ tilt angle $\theta(i,j) = \Delta\theta$



$$\Rightarrow E_{\text{ex},ij} = -2JS^2 \cos(\Delta\theta) \approx -2JS^2 \left[1 - \frac{(\Delta\theta)^2}{2} \right] = \text{const.} + JS^2 a^2 (\partial_x \theta)^2$$

$$\text{In 3D: } e_{\text{ex}} = \frac{A(\nabla \vec{M})^2}{M_s} \Rightarrow E_{\text{ex}} = \frac{A}{M_s^2} \int (\nabla \vec{M})^2 dV \text{ w/ } A \text{ "exchange stiffness const."}$$

for cubic lattice: $A = n \frac{3S^2}{a}$, $n=1, 2, 3$
simple bcc, fcc

C. Magnetostatic (self-field) energy

Interaction of magnetization w/ self induced demagn. field \vec{H}_d

$$\nabla \cdot \vec{H}_d = -\nabla \cdot \vec{M}$$

$$\Rightarrow E_{ms} = -\frac{1}{2} \mu_0 \int_V \vec{H}_d \cdot \vec{M} dV \quad | \quad \vec{B} = \mu_0 (\vec{H}_d + \vec{M}) \\ = \frac{1}{2} \mu_0 \int_V \vec{H}_d^2 dV$$

homogeneously magnetized ellipsoids: $\vec{H}_d = -\hat{N} \vec{M}$ w/ $\hat{N} = \begin{pmatrix} N_x & 0 & 0 \\ 0 & N_y & 0 \\ 0 & 0 & N_z \end{pmatrix}$

Thin film $\vec{m} \parallel \hat{e}_z$: $N_x = N_y = 0, N_z = 1$

Sphere: $N_{x,y,z} = \frac{1}{3}$

Cylinder $\vec{m} \parallel \hat{e}_z$: $N_x = N_y = \frac{1}{2}, N_z = 0$

$$w/ \vec{m} = \frac{\vec{M}}{M_s}, \vec{h}_d = \frac{\vec{H}_d}{M_s} \Rightarrow E_{ms} = -\underbrace{\frac{\mu_0 M_s^2}{2}}_{K_d \text{ dipolar const.}} \int_V \vec{h}_d \cdot \vec{m} dV$$

$$\Rightarrow \text{Magn. stat. dens. } e_{ms} = -K_d \vec{h}_d \cdot \vec{m}$$

D. Magn. anisotropy energy

orientation dep. contribution of magnetization to internal energy

\vec{M} along easy axis $\Rightarrow E_A \text{ min.}$

$$e_A = K_A f(\phi, \psi)$$

Different types of anisotropy:

(i) shape anisotropy

associated w/ surface \rightarrow shape of sample

$$e_{sh} = -\frac{\mu_0 M_s^2 \sin^2 \theta}{2} = -K_d \sin^2 \theta \quad \text{"energy required to rotate magnetization"}$$

(ii) Magnetocrystalline anisotropy

2

(ii) Magnetocrystalline anisotropy

Causes preferred alignment of magn. to certain cryst. direction

$$\text{Simplest case: } e_{mc} = K_1 \sin^2 \theta + K_2 \sin^4 \theta + \dots$$

$\hookrightarrow \vec{M} \neq \vec{M}_{\text{easy axis}}$

(iii) Surface anisotropy

Due to reduced number of neighbours

$$e_{su} = K_{su} \sin^2 \theta \quad \Rightarrow \quad \int dA$$

$\hookrightarrow \vec{M}_{\text{surf}}$

Comparison to surface density: $e_{sh} = -K_d \sin^2 \theta$; $e_{su} = K_{su} \sin^2 \theta$

$$\Rightarrow e_A = - \left(K_d - 2 \frac{K_{su}}{d_f} \right) \sin^2 \theta$$

K_{eff}

$$\text{From shape \& surface anisotropy} \Rightarrow M_{\text{eff}} = M_s \frac{K_{\text{eff}}}{K_d} = M_s - \frac{4K_{su}}{M_0 M_s} \frac{1}{d_f}$$

D. Total energy & characteristic quantities

With all e 's:

$$\begin{aligned} E_{\text{tot}} &= \int_V \left\{ A \left(\frac{\nabla \vec{M}}{M_s^2} \right)^2 + K_A e_A(\theta, \varphi) - \frac{M_0}{2} \vec{M} \cdot \vec{H}_d - M_0 \vec{M} \cdot \vec{H}_{\text{ext}} \right\} dV \\ &= K_d \int_V \left\{ \frac{A}{K_d} \left(\nabla \vec{m} \right)^2 + \frac{K_A}{K_d} e_A(\theta) - \vec{m} \cdot \vec{h}_d - 2 \vec{m} \cdot \vec{h}_{\text{ext}} \right\} dV \\ &\quad \text{=: } l_{\text{ex}} \quad \text{=: } \chi \text{ "hardness param."} \\ &= \frac{2A}{M_0 M_s^2} \end{aligned}$$

$$\Rightarrow \text{Bloch param } \Delta = \frac{l_{\text{ex}}}{\sqrt{\chi}} = \sqrt{\frac{A}{K_d}}$$

$$\Rightarrow \text{Thickness of domain wall: } \delta_v = \pi \sqrt{2} \Delta$$

$$\Rightarrow \text{Crit. domain dia.: } D_{\text{cr}} = 36 l_{\text{ex}} \sqrt{\chi}$$

5.3.2 Magnetic Domains

Bloch wall: Magnetization rotates within the wall plane



Néel wall: Magn. rotates within film plane, perpendicular to domain wall

Domain wall thickness grain

Consider N lattice planes w/ lattice spacing a

$\rightarrow \Delta \theta = \frac{\pi}{a} = \text{const.}$ for magn. between planes

$$\Rightarrow e_{ex} = \frac{\pi^2 A}{a N}, \quad e_A = \frac{K_A N}{2}, \quad e_{dw}(N) = e_{ex}(N) + e_A(N)$$

$$\Rightarrow \delta_v = N a = \pi \sqrt{2} \sqrt{\frac{A}{K_A}}$$

\rightarrow

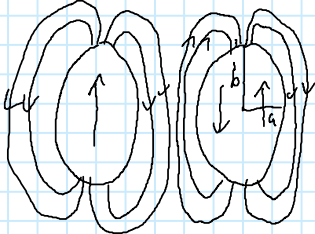
$$\Rightarrow S_0 = N a = \pi \sqrt{2} \sqrt{\frac{A}{K_d}}$$

$$\Rightarrow \text{Energy dens. of wall } e_{dw} = \pi \sqrt{2} \sqrt{A K_d}$$

$$\Rightarrow \theta(x) = 2 \arctan \left\{ e^{\frac{x}{\Delta}} \right\} \quad \text{w} \quad \Delta = \sqrt{\frac{A}{K_d}} \quad (\text{Domain wall at } x=0, e_{dw} = 4 \sqrt{A K_d})$$

Critical single-domain size

- Compare single-domain state to two-domain state of ellip. part. and search for crit size, same en. in both states



$$\text{Single Dom.: } V = \frac{4}{3} \pi a^2 b, \text{ demagn. fact. } N_{ii}$$

$$\Rightarrow E(1) = E_{ms}(1) = -\frac{1}{2} M_0 \vec{H}_d \vec{M} \cdot V = N_{ii} K_d \cdot \frac{4}{3} \pi a^2 b$$

Two Dom.:

$$E(2) = E_{ms}(2) + E_{dw} = \alpha N_{ii} K_d \cdot \frac{4}{3} \pi a^2 b + \pi a b e_{dw}$$

$$E(1) = E(2)$$

$$\Rightarrow D_{cr} = 2a = \frac{3}{2N_{ii}(1-\alpha)} \frac{e_{dw}}{K_d} \quad | e_{dw} = 4 \sqrt{A K_d}, a=b, N_{ii} = 1/3, \alpha \approx 1/2$$

$$= 36 \frac{\sqrt{A K_d}}{K_d}$$

5.4 Magnetic Nanoparticles (MNPs)

5.4.1. Basics

Drastic change in hysteresis loop

Problem of char.

Small V \rightarrow small signals

When ensemble:

- interactions of MNPs
- No info for magn. anisotropy of single MNP
- Only average properties

Magnetic Moments of 3d transition met. nanopart.

Behavior of MNP more like atom. In this limit magn. mom. $\rightarrow M_B$

Single Dom part.

Size $D < D_{crit} \Rightarrow$ formation of Dom wall unfavorable \rightarrow Single Dom state

Magnetization reversal via coherent rot. of their spins

Stoner-Wohlfarth model

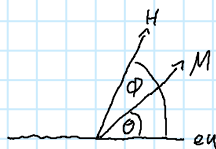
Ideal homogeneous alignment of all spins: $|\vec{M}| = \text{const.} = M_s$

\rightarrow Exchange en $E_{\text{ex}} = \text{const.}$

Anisotropic systems: E_{aniso} vs. E_z (Zeeman)

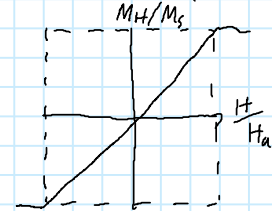
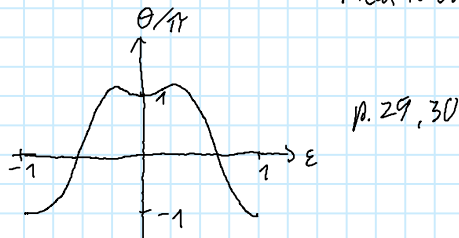
$$E = K_1 V \sin^2 \theta \sim \mu_0 H M_s V \cos(\theta - \phi)$$

from $M \downarrow \perp H$ both to easy axis



$$\text{Introduce anisotropy field } H_a = \frac{2K_1}{M_0 M_s}, \quad \varepsilon = \frac{E}{K_1 V}, \quad h = \frac{H}{H_a}$$

$$\Rightarrow \varepsilon = \sin^2 \theta + 2h \cos \theta$$



Field to overcome barrier and switch in other state

Superparamagnetic limit

Single domain at $H=0$ $M \parallel \text{ea}$, two states diff by 180° with equal energy separated by en barrier $K_1 V$, reversal of M induced by thermal activation over barrier

\Rightarrow Relaxation time $\tau = \tau_0 \exp\left(\frac{K_1 V}{k_B T}\right)$ T can reach from $.14 s - 2 \cdot 10^7 s$

$$\text{Measuring/Dr time } \tau_i \Rightarrow \text{Blocking temp. } T_B = \frac{K_1 V}{k_B \ln\left(\frac{\tau_i}{\tau_0}\right)}$$

Ferrofluids p. 31

5.4.2 MNP Applications

- ferrofluids
- high-density information storage
- magn. resonance imaging (MRI)
- biol. cell labeling, sorting & separation of biochem.
- targeting & drug delivery

Mostly MNPs out of $\text{Fe}_x \text{O}_y$ particles

5.4.3 Magnetic Nanowires

Ext. magn. Field \vec{H}

Apply Stoner-Wohlfarth model

$$N_x = N_y = N_{\perp} = \frac{1}{2}, \quad N_z = N_{\parallel} = 0$$

$$\Rightarrow E_{\text{sh}} = \frac{4}{4} \frac{M_0}{K_{\text{sh}}} M_s^2 V \sin^2 \theta$$

$$+ E_{\text{mc}} = K_{\text{mc}} \sin^2 \theta$$



$$K_{sh} \\ + E_m = K_m \sin^2 \theta$$

$$\Rightarrow K_1 = K_m + K_{sh}$$

$$\Rightarrow E = K_1 V \sin^2 \theta - M_0 H M_s V \cos(\theta - \varphi)$$



Switching field H_{sw} :

$$K_{sh} \gg K_m, K_1 \approx K_{sh}, \phi = \pi$$

$$\Rightarrow H_{sw} = H_a = \frac{2K_1}{M_0 M_s} \approx \frac{M_s}{2}$$

Alternative: Carling

$$D > D_{cr}^{curl} = \pi L_{ex} \Rightarrow \text{Carling mode energetically most favourable}$$

Magnetization tangentially to surf $\Rightarrow E_{sh} \downarrow$

$$\Rightarrow H_{sw} = a \cdot \frac{M_s}{2} \quad \text{w} \quad a = 6.78 \left(\frac{2L_{ex}}{D} \right)^2$$

For $D > D_{cr}^{curl} \Rightarrow a < 1$

5.5 Magnetism of thin films & Multilayer

Spin-dep scattering, spin-dep. tunneling importante

5.5.1 Magnetoelectronics / Spintronics, 'MR-effects'

Spintronics: Exploit the fact that e^- carry magn. mom ($\uparrow\downarrow$ spin) in addition to el. charge

$$MR = \frac{R(H) - R(0)}{R(0)} = \frac{\Delta R}{R(0)} \quad \text{"Magnetoresistance" w.r.t. R: el. res., H: Magn. field}$$

New developments:

- Giant MR effect:
magn coupling & spin-dep. scat.
- Colossal MR effect
- Tunneling

5.5.2 GMR

Layer system w.r.t antiparallel, parallel magnetization
(a) (p)

\vec{H}
(a) \rightarrow (p) \Rightarrow Resistance \downarrow

$$GMR = \frac{R_a - R_p}{R_p}$$



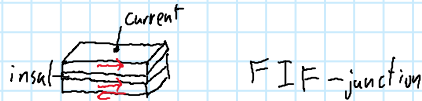
Spin dependent scat. w.r.t subbands of minority ($\downarrow\uparrow$ M) & majority ($\uparrow\uparrow$) spins

—
Parallel alignment of magnetization

$$\text{Spin } \downarrow: E_n = \frac{\hbar^2}{2m} \left(\frac{n\pi}{a_n} \right)^2 + \frac{\hbar^2}{2m} (k_x^2 + k_y^2) + V$$

$$\text{Spin } \downarrow: E_n = \frac{\hbar^2}{2m} \left(\frac{n\pi}{d_N} \right)^2 + \frac{\hbar^2}{2m} (k_x^2 + k_y^2) + V$$

5.5.3 Tunnel magneto resistance (TMR)



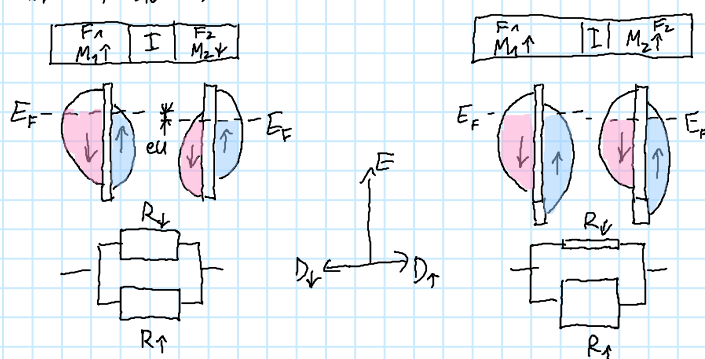
$$TMR = \frac{R_u - R_p}{R_p}$$

$$\text{Spin polarization: } P = \frac{D_{\text{mag}}(E_F) - D_{\text{min}}(E_F)}{D_{\text{mag}}(E_F) + D_{\text{min}}(E_F)} = m - (1-m) = 2m-1 \quad \text{"Asymm. of ↑ & ↓ Fermi-level"}$$

Julliere model for FIF-junctions

Ass.:

- Elastic tunneling
- Spin conservation (No spin flip)
- $G_{\uparrow} \propto D_{1,\uparrow}(E_F) D_{2,\uparrow}(E_F)$
- $G_{\downarrow} \propto D_{1,\downarrow}(E_F) D_{2,\downarrow}(E_F)$



Zusammenfassung Chapter06

Donnerstag, 28. Juli 2022 15:55

6. Carbon nanostructures

Different allotropes:

- 3D: Diamond & graphite
- 2D: Graphene
- 1D: Carbon nanotubes
- 0D: (Buckminster) fullerenes (spherical configs)

6.1 Graphene

Honeycomb structure, $a_0 = 1.42 \text{ \AA}$ "shift betw. two triangular sub-lattices"

Properties:

- High therm-cond.
- High mech stability
- High surf/vol ratio
- Light
- :

El. properties

- Excellent cond. w/ high el. cond.
- Universal cond. min. of $\sigma = \frac{4e^2}{h}$
- :

Zero bandgap semicond w/ $E_F = 0$

Close to E_F linear Dispersion,

$$E(\vec{k}) = \hbar v_F |\vec{k} - \vec{k}_F| \quad \text{w/ } v_F \approx 10^6 \text{ m/s (eff. speed of light)}, \vec{k}_F: \text{Dirac points}$$

Dispersion by tight binding model:

$$\vec{a}_1 = a \left(\frac{1}{2}, \frac{\sqrt{3}}{2} \right), \vec{a}_2 = a \left(-\frac{1}{2}, \frac{\sqrt{3}}{2} \right) \quad \text{w/ } a = \sqrt{3} a_0 \text{ "above & spacing to neighbouring atoms"}$$

$$\text{Ansatz: } \psi_{\vec{k}} = \sum_{\vec{R} \in G} e^{i \vec{k} \cdot \vec{R}} \phi(\vec{x} - \vec{R}) \quad \text{w/ } G: \text{lattice vect. space, } \phi(\vec{x}) \text{ atomic WF}$$

Per cell two p_z -orbitals ϕ_1, ϕ_2 at $\vec{x}_1, \vec{x}_2 \Rightarrow \phi(\vec{x}) = b_1 \phi_1(\vec{x}) + b_2 \phi_2(\vec{x})$

$$\text{Single } e^- \text{ in pot. of C atoms at } \vec{x}_1, \vec{x}_2: \quad H = \frac{\vec{p}^2}{2m} + \sum_{\vec{R} \in G} (V_{\text{at}}(\vec{x} - \vec{x}_1 - \vec{R}) + V_{\text{at}}(\vec{x} - \vec{x}_2 - \vec{R}))$$

$$\delta H \phi_{1,2} = E_{1,2} + \Delta U_{1,2} \phi_{1,2}$$

$\hookrightarrow E_1 = E_2$ eigen vals of ρ_2 states

$$\Delta U_1 = \sum_{\vec{R} \neq 0} (V_{at}(\vec{x} - \vec{x}_1 - \vec{R}) + V_{at}(\vec{x} - \vec{x}_2 - \vec{R}) + V_{at}(\vec{x} - \vec{x}_3 - \vec{R}))$$

$$\text{Choose } E_{1,2} = 0 \Rightarrow H \phi_{1,2} = \Delta U_{1,2} \phi_{1,2}$$

$$H \psi_{\vec{k}} = E(\vec{k}) \psi_{\vec{k}} \text{ by projec. } E(\vec{k}) \langle \phi_j | \psi \rangle = \langle \phi_j | \Delta U_j | \psi \rangle$$

$$\text{Be } \gamma_0 = \int \phi_1^* \phi_2 = \int \phi_2^* \phi_1, \epsilon \in \mathbb{R}, \gamma_1 = \int \phi_1^* \Delta U_1 \phi_2 = \int \phi_2^* \Delta U_2 \phi_1$$

$$\Rightarrow p. 5, (6.2-5) \text{ w abbreviation } \alpha(\vec{k}) = (1 + e^{-ik\vec{a}_1} + e^{-ik\vec{a}_2}), \alpha^* = \dots$$

$$\Rightarrow \text{EW-problem w } \gamma_0 \approx 0 \Rightarrow E(\vec{k}) = \dots \quad (6.6) \text{ p. 5}$$

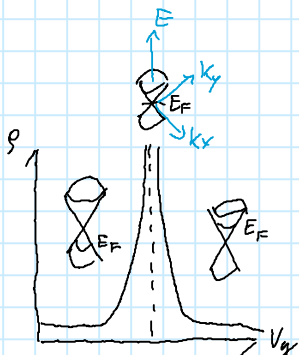
$$\text{Note that: } E(\vec{k}_i) = 0$$

By doping/impurities $\Rightarrow E_F$ opened \rightarrow SC like behaviour.

By pos. or neg. volt. \Rightarrow chem. pot. shifted into CB or VB

\Rightarrow Accumulation of $e^- \rightarrow$ CB or $h \rightarrow$ VB

\Rightarrow n- or p cond. "Ambipolar"



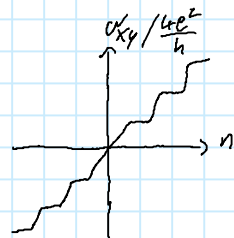
$$\text{Cond. } \sigma_{min} = \frac{4e^2}{h} \Rightarrow \sigma_{max} = \frac{h}{4e^2}$$

Shubnikov de Haas 4-fold degenerated (2 spin + 2 valley)

$$\text{QHE cond. quantized in } \frac{4e^2}{h} \left(N + \frac{1}{2} \right)$$

At $E=0$: only pseudo spin accommodated

In two layer graphene again $\Delta \sigma_{xy} = \frac{4e^2}{h}$ but $\frac{4e^2}{h} N$ w graph of $\frac{8e^2}{h}$ around $n=0$



Preparation & structuring

- Scotch tape
- Thermal decompos. of SiC at 1000-1500°C, Si sublimated from Surf and on the top forms a C-layer
- Chem. vapour deposition: single cryst. catalyst layer (eg Cu, Ni) heated up, C containing gases decomposed at surf
- Other

Other 2d layer structures

- Mimick graphene by other building blocks
- Transition metal dichalcogenides (TMDs)

6.2 Carbon nanotubes (CNTs)

Three types: indices $[n:m:0]$ Θ metallic

Three types: indices (n, m, θ) metallic

zig-zag	$(n, 0)$	0°	?
armchair	(n, n)	30°	✓
chiral	$m \notin \{0, n\}$	$0^\circ < \theta < 30^\circ$?

BUT

CNTs described by chiral indices (n, m)

Every atom can be reached by $\vec{C}_k = n\vec{a}_1 + m\vec{a}_2$

$$a_{c-c} = a_0 = 1.42 \text{ \AA}$$

$$|\vec{a}_1| = |\vec{a}_2| = a = 2.46 \text{ \AA}$$

$$d = \frac{a}{\pi} \sqrt{n^2 + m^2 + mn} \quad \text{distance}$$

$$\tan \theta = \frac{\sqrt{3}m}{2n+m} \quad \text{chiral angle } \theta \text{ for } \vec{a}_1 \text{ & } \vec{C}_k$$

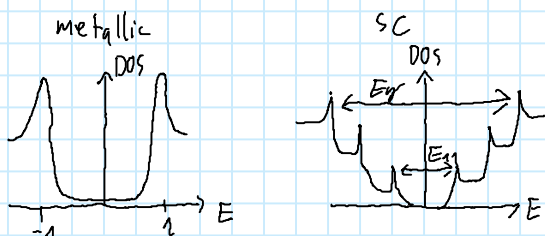
$$\left. \begin{array}{l} \frac{n-m}{3} \in \mathbb{N}, \text{ metallic, all armchairs} \\ \frac{n-m}{3} \notin \mathbb{N}, \text{ semicond} \end{array} \right\} \Rightarrow \frac{2}{3} \text{ sc, } \frac{1}{3} \text{ met}$$

Multi-walled CNTs: One metallic \rightarrow Multi met.

1D CNT: k-rec. quantized

\Rightarrow For $E(\vec{k}), \vec{C}_k : \vec{k} \cdot \vec{C}_k = 2\pi n, n \in \mathbb{N}$

\Rightarrow Sharp peaks called van Hove singularities



Prep. of CNTs

- Chem. vapour deposition
 - substrate w/ patterned catalyst in oven, C containing gas inside
 - single walled w/ nm-scale catalyst dot
 - bottom growth (Fe) or at tip (Ni)
- Arc discharge
 - Gas filled space betw. two C electrodes
- Laser ablation:
 - Vapourize C from graphite target

Device application

- conducting channel in transistors, as field emitters FTV
- Carbon fiber in sports equipment

6.3 Buckminster fullerenes

Spherical config w $\approx 20 - 200$ C atoms

Special: C_{60} Buck-balls ordered in pentagons & hexagons

Endohedral fullerenes: Structure filled w other elements

Prep. by laser/arc discharge evaporation of graphite

Used as acceptors in organic solar cells

6.4 Raman spectroscopy

• Chemical fingerprint

• Char. energy diff. betw. incident & re-emitted light due to molecular vibrations in mat.

- En. loss "Stokes shift"

- Already vib. in ground state transferred to γ "Anti-Stokes" ↑ Sym. in wavenumber

↳ lower intensity

$$\text{Raman shift} = \Delta\tilde{\nu} = \frac{1}{\lambda_0} - \frac{1}{\lambda_1} = \frac{E_0 - E_1}{hc}$$

Raman modes:

G-peak: Optical in-plane Raman mode, sp^2 -C-C vib.; p-dop \rightarrow blueshift, n-dop \rightarrow red shift

D-peak (defect peak): Radial breathing mode, rad. osci of C-ring

2D-peak: 2x wavenumber of D-peak, involves two phonon processes

$$\# \text{graphene sheets} \hat{=} I_{2D}/I_G$$

Abb p.20 (6.27)

Additional peaks due to impurities or defects \rightarrow high defect, lower quality graphene

Raman spectra of CNTs

Radial breathing modes: at low wavenumbers, char. for each CNT

$$\Delta\tilde{\nu}_{RBM} = \frac{c_1 + c_2}{d}$$

Zusammenfassung Chapter07

Dienstag, 2. August 2022 12:49

07 Preparation

7.1 Thin film growth: Concepts & Theory

7.1.1 Categories

- Frank van der Merwe (FM) growth
layer by layer \sim completely wetting
- Stranski - Krastanov (SK) growth
Layer by layer, then islanding \sim intermediate case of "spreading scenarios"
- Vollmer - Weber (VW) growth
islanding \sim dewetting (finite wetting angle)

Which case occurs is related to the surface/interface tension γ

$$\gamma_{\text{surf}} = \gamma_{\text{film}} + \gamma_{\text{sf}} \cos \phi$$



| Only kinetic analogy!

$$\Rightarrow \text{Wetting angle FM: } \phi = 0 \quad \gamma_s \geq \gamma_f + \gamma_{sf}$$
$$\text{VW: } \phi > 0 \quad \gamma_s \leq \gamma_f + \gamma_{sf}$$

7.1.2 How to describe Growth?

Dynamic problem

- Time scales of incoming atoms/mols \sim growth rate
- Time scales of dynamics on growing surf (e.g. diffusion)

7.1.3 Simple Growth Models

7.1.3.1 Langmuir growth for a monolayer

- Absorbate grows only in monolayer \sim thiols on gold type

Rate of change of coverage Θ : $\frac{d}{dt} \Theta = \frac{1}{\tau} (1-\Theta) \quad \text{w solution } \Theta(t) = 1 - \exp^{-t/\tau}$

\hookrightarrow growth rate

7.1.3.2 Multilayer Growth without interlayer Diffusion ("Statistical Growth")

All layers w their respective Θ_n

No diffusion

$$\underline{\Delta \Theta_n = \Omega F (\Theta_{n-1} - \Theta_n)} \quad \text{w F: Flux, } \Omega \cdot \text{absorption, w cond. } \Theta_0 = 1$$

No diffusion

$$\frac{d}{dt} \Theta_n = -\Omega F (\Theta_{n+1} - \Theta_n) \quad \text{w F: Flux, } \Omega \cdot \text{absorption, w cond. } \Theta_0 = 1$$

Exposed layer coverage: $\varphi_n = \Theta_n - \Theta_{n+1}$

$$\text{Solution: } \Theta_n = 1 - e^{-\theta} \sum_{k=0}^{n-1} \frac{\theta^k}{k!} \quad \text{w total coverage } \Theta = \sum_{n=1}^{\infty} \Theta_n = -\Omega F t \quad \text{w } 0 \leq \Theta_n \leq 1$$

φ_n follows Poisson dist.

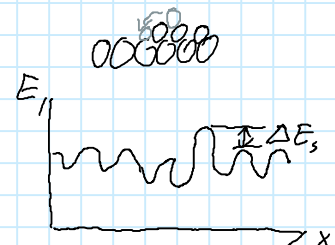
$$\varphi_n = \frac{e^{-\theta} \theta^n}{n!} \quad \rightarrow \text{Variance } \text{Var} = \theta \approx \text{roughness}$$

7.1.4 Intralayer & Interlayer Diffusion & Ehrlich-Schwoebel Barrier

- Intralayer diff D (within one layer) \rightarrow typ. island size
- Interlayer diff D' (multiple layers)

$$D = D_0 \exp\left(-\frac{E_D}{k_B T}\right)$$

$$\frac{D'}{D} = \exp\left(-\frac{\Delta E_s}{k_B T}\right) \ll 1 \quad \text{w } \Delta E_s: \text{Ehrlich-Schwoebel barr.}$$



Appendix: Langmuir isotherm

7.1.5 Nucleation Theory

7.1.5.1 Classical (Continuum) Nucleation theory

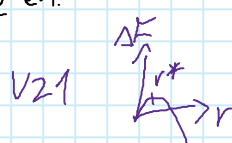
3D nucleation:

after formation of a nucleus \rightarrow New mat. of environment can diffuse and attach to nucleus

\rightarrow Change in free energy:

$$\Delta F = \Delta F_{\text{vol.}} + \Delta F_{\text{surf.}} = \frac{4\pi}{3} r^3 \Delta g_v + 4\pi r^2 \gamma^* \quad \begin{matrix} \text{Volume part} \\ \text{Interface en.} \end{matrix}$$

$$\text{Nucleus stable for } r > r^* \quad \text{w } r^* = \frac{2\gamma^*}{\Delta g_v}$$



2D nucleation

e.g. 2D islands

7.1.5.2 Atomistic Nucleation theory

$$\text{Copy \& paste in script} \rightarrow l_s \sim \left(\frac{D}{F}\right)^{1/6}$$

7.1.6 Island shapes

7.1.6.1 Equilibrium Island shapes

7.1.6.1 Equilibrium Island shapes

Wulff construction - minimization of surf. en.

Isotropic sys \rightarrow circular shape

Crystalline sys \rightarrow cryst. symmetry

For heteroepitaxy \rightarrow strain due to lattice mismatch

7.1.6.2 Fractal-Dendritic Islands

e.g. Snowflakes

7.1.6.3 Diffusion-Limited Aggregation (DLA)

Weird random growth model

7.1.7 Pictures

7.1.8 Statistical Description of surfaces by correlation functions

Surface width or root-mean-squared roughness

$$\sigma = \sqrt{\langle [h(x,y) - h(x_i,y_i)]^2 \rangle} \quad \text{w.r.t. } (x-x_i), (y-y_i) \rightarrow \infty$$

↳ average

\Rightarrow Height diff. correlation function

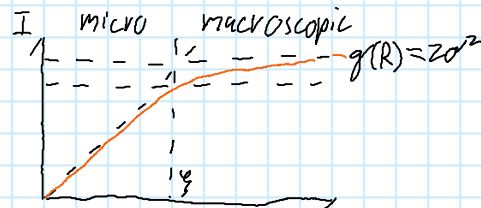
$$G(r) = \langle [h(x+r) - h(x)]^2 \rangle$$

w.r.t. height-height-corr-fct.

$$C(r) = \langle [h(x+r) h(x)] \rangle$$

$$\Rightarrow G(r) = 2\sigma^2 - 2C(r)$$

often used: $C(r) = \sigma^2 \exp\left[-\left(\frac{r}{\xi}\right)^{2\alpha}\right]$



7.1.9 Notes on Background of scaling Laws in growth physics & self-affinity

-

Skip until anti Bragg